NETWORK APPROXIMATION IN THE LIMIT OF SMALL INTERPARTICLE DISTANCE OF THE EFFECTIVE PROPERTIES OF A HIGH CONTRAST RANDOM DISPERSED COMPOSITE.

LEONID BERLYAND * AND ALEXANDER KOLPAKOV †

Abstract.
We consider a high contrast two phase composite such as a ceramic/polymer composite or a fiberglass composite. Our objective is to determine the dependence of the effective conductivity $\hat{A}$ (or the effective dielectric constant or the effective shear modulus) of the composite on the random locations of the inclusions (ceramic particles or fibers) when the concentration of the inclusions is high. We consider a two dimensional model and show that the continuum problem can be approximated by a discrete random network (graph). We use variational techniques to provide rigorous mathematical justification for this approximation. In particular, we have shown asymptotic equivalence of the effective constant $\hat{A}$ for the discrete and continuum models in the limit when the relative interparticle distance goes to zero. We introduce the *geometrical interparticle distance parameter* using Voronoi tessellation, and emphasize the relevance of this parameter due to the fact that for irregular (non periodic) geometries it is not uniquely determined by the volume fraction of the inclusions.

We use the discrete network to compute $\hat{A}$ numerically. For this purpose we employ a computer program which generates a random distribution of disks on the plane. Using this distribution we obtain the corresponding discrete network. Furthermore the computer program provides the distribution of fluxes in the network which is based on the Keller's formula for two closely spaced disks. We compute the dependence of $\hat{A}$ on the volume fraction of the inclusions V for monodispersed composites and obtained results which are consistent with the percolation theory predictions. For polydispersed composites (random inclusions of two different sizes) the dependence $\hat{A}(V)$ is not simple and is determined by the relative volume fraction V_r of large and small particles. We found some special values of V_r for which the effective coefficient is significantly decreased. The computer program which is based on our network model is very efficient and it allows us to collect the statistical data for a large number of random configurations.

Key words. asymptotics, interparticle distance parameter, high contrast, homogenization, network approximation, polydispersity, percolation, random composite.

AMS subject classifications. 15A15, 15A09, 15A23

Introduction. We consider a problem of determining effective properties of a two phase composite material in which a large number of small particles is *randomly* distributed in a homogeneous medium (a matrix or a host with dispersed filler). We consider the case when properties of the matrix and the filler are vastly different. This question arises in a variety of engineering problems.

We next present three examples, which motivated our work.

Optimal design of electrical capacitors. It is well known that the capacity of an electrical capacitor is proportional to the dielectric constant [39]. Most of the materials have the dielectric constant which is not too large, usually no greater than 10 (in relative units). On the other hand several kinds of ceramic materials have an extremely high dielectric constant ($10^3 - 10^4$ or even higher) [25]. However, in many situations it is not practical to use pure ceramic as a principal element of a capacitor because ceramic has unsatisfactory mechanical properties (too brittle). Therefore a composite of a matrix with a low dielectric constant (which provides the desired mechanical properties) and ceramic particles (which increase the effective dielectric constant) is typically used in industry. Practical issues in the design of such

* Penn State University, Department of Mathematics, University Park, PA 16802 & Department of Mathematics and Computer Science, University of Akron, (berlyand@math.psu.edu).

† 324 Bdl.95, 9th November str., 630009, Novosibirsk, Russia

composites is selection of the filler identity, size distribution and optimal array of the filling particles.

Thermal management in the electronics industry. Modern integrated circuit design needs highly efficient "packages"(composites) for heat removal. This need is driven by the fact that modern circuits have more "elements" per volume (to miniaturize the devices and make them more powerful) and therefore they generate more heat per volume. A typical package is a compound of an epoxy based polymer filled with ceramic (or other highly conductive material) powders so that the ratio of the thermal conductivities is of order of 10^2 ([18]). The rational behind using such composites is the same as for the electrical capacitors; epoxy based polymers provide desired mechanical properties while the filler increases the heat conductivity.

Mechanical properties of fiber reinforced composite materials. Calculation of the effective shear modulus of a transversely-random unidirectional composite of parallel fibers (e.g. fiberglass composites) is based on the solution of a Laplace type PDE (more precisely antiplane elasticity vectorial problem amounts to solving one scalar PDE). The coefficients in this equation have meaning of stiffness of the matrix and the fibers. For modern composites the contrast ratio is again quite high, for example, in the case of the boron fibers in epoxy matrix it is about $200 - 400$ ([26]).

All the above problems (the list of examples can be continued) have two main features: *random* microstructure and *high contrast* in physical properties. Rigorous mathematical results on homogenization of random microstrusture were obtained in classical works [23], [34]. In these works the existence of the homogenized limit under very generic assumption on the microstructure has been rigorously proved. Rigorously justified explicit computational formulas are available only for a few special structures [20], [13]. Some heuristic computational formulas and mixing rules, which are based on physical considerations (see for example, [10] where a number of such formulas for the effective dielectric constant are presented), are in reasonably good agreement with experimental data only in a certain range of parameters and this range is typically either not known or quite restrictive (e.g. small concentration).

A variety of rigorously justified bounds on the effective properties of composites has been obtained over recent years (see [28] for the review on bounds). For high contrast composites the bounds from [11] work well below the percolation threshold.

It is also possible to calculate effective properties of random high contrast composites using numerical methods by solving directly the PDEs with rapidly oscillating coefficients (e.g. finite elements or integral equations, see for example, [2], [15]). Then two questions arise. The first is how large is the dimension of the problem (since the problem is highly inhomogeneous, the corresponding grid has to have a large number of grid points). The second is how to take into account the high contrast of the composite phases. In particular, it is necessary to address the issue of concentrated fluxes between closely spaced inclusions which requires the use of a very fine mesh in the domains of concentration (see also [42] for analytical study of the concentration phenomenon). It leads to further increase of the complexity of the problem. Finally, it is necessary to repeat this computation and average over a large number of random configurations (i.e. to collect statistics). All these makes the problem very difficult.

We propose a different approach that approximates the continuum problem with a discrete network connecting neighboring particles. The notions of a neighbor and a neighborhood of a particle play essential role in our consideration. We introduce these notions using Voronoi tessellation (see below) which leads to a natural definition of the neighboring particles (disks) and the "boundary" disks that is disks which lie

near the external boundary. We observe that while for periodic structures the volume fraction of the particles uniquely determines the distances between the particles, this is no longer true for irregular structures and one should search for a new *interpartilce distance parameter*, which describes the local geometry when the inclusions are close to touching. We introduce the interparticle distance parameter for highly packed composites using Voronoi tessellation and obtain a rigorous asymptotic approximation with respect to this parameter.

We also remark that the domains of the flux concentration in some sense determine the effective properties (this will be shown in our analysis). That is why the computation of the solution outside these domains does not provide useful information but leads to an essential increase in the complexity of the problem. This further motivates our interest in developing a relatively simple (suitable for collecting statistical data in numerical experiments and capturing the percolation effects) and at the same time rigorously justified model of a random composite. Note that the high contrast in physical properties is essential in our consideration and in the case of an arbitrary contrast ratio (not necessarily high) the corresponding analysis becomes much more cumbersome.

We consider a medium with piecewise constant characteristics, which corresponds to a two phase composite. Highly conducting inclusions are replaced by the ideally conducting inclusions (with infinite conductivity). This approach is in agreement with bounds [11] which imply that if the contrast ratio is greater than several hundreds, then for many practical purposes it can be taken to be infinite. More precisely if one plots the effective conductivity versus the contrast ratio using formulas from [11], then the curve becomes almost horizontal after the contrast ratio reaches certain value (2000-3000 for typical polymer/ceramic composites).

Finally we mention that our approach allows to obtain an analytical error estimate in which all constants are explicitly defined. This estimate will be presented in the forthcoming paper [7].

We now present an overview of the paper. In the section 1 we introduce a discrete network model which corresponds to a continuum two phase composite of a matrix and particles or fibers (0-3 or 1-3 composites, [32]) (subsections 1.1 and 1.2).

The network model is a system of Kirchhoff's type on a graph with appropriate boundary conditions. The sites of the graph correspond to the particles and the values of (local) fluxes between nearest particles are assigned to the edges of the graph. These values are the key parameters of the model and we use the Keller's formula [20] (see also [37]) to compute the local fluxes between the neighboring disks (which corresponds to the cross section of the fibers). We also obtained an algebraic formula for the effective conductivity, which corresponds to the network model (subsection 1.3).

We implemented a computer program for solving the proposed discrete model. It takes a reasonable amount of time and it allows us to perform several thousand runs to obtain the statistical data and to compute physical parameters averaged over a large number of random arrays of the inclusions (filler).

In subsection 1.4 we use our model to solve numerically the problem for a monodispersed (random inclusions of the same size) and polydispersed (random inclusions of two different sizes) filler. For the monodispersed filler we obtain the dependence of the effective coefficient $\hat{A}$ on the volume fraction V of the filler which agrees with theoretical predictions based on the percolation theory considerations.

For the polydispersed case the dependence of the effective coefficient $\hat{A}$ on the

volume fraction V of the filler is not simple and is determined by the relative volume fraction V_r of large and small particles. There are some special values of V_r for which the effective coefficient is decreased by factor two, see Fig. 1.6. The latter shows an interesting new feature of the high-contrast closely-packed composites and sheds light on the important practical question: how one should grind the filling powder for such composites. We provide a comparison of this result with the dilute irregular case and the periodic closely packed case and observe that the polysipersity effect is much more pronounced and qualitatively different in the highly packed irregular high contrast composites. We also note that mathematical understanding and justification of this effect poses a challenging open problem for mathematicians working on percolation theory.

Section 2 is devoted to the derivation and mathematical justification of the discrete network approximation.

We remark here that the discrete circuit (network) models for various high contrast models have been used extensively in physics literature ([1],[12],[17],[22],[35] ,[36]. However, the relationship between the original continuum model and the corresponding discrete problem have not been analyzed mathematically. In the work [24] high contrast conductivity problems were first formulated and analyzed using variational methods. In [24] an asymptotic analysis in the high contrast ratio parameter had been carried out for a random checkerboard model, which can be reduced to a lattice percolation problem. Note that in our case there is no high contrast parameter (the contrast is infinitely large). Moreover our asymptotic analysis is done with respect to the geometrical interparticle distance parameter and there is no underlying lattice percolation in our problem. The latter means that our problem should be described using continuum percolation models. In the work [9] L. Borcea and G. Papanicolaou pioneered rigorous mathematical characterization of electro-magnetic properties of high contrast, continuous problems using the network approximation and asymptotics in the high contrast ratio parameter. They introduced an idea of using the Kozlov's solution([24]) at a saddle point as a basic building block of the network. This allows to express the effective conductivity in terms of the principal curvatures at the saddle points of the phase functions. Their results apply to a large class of inhomogeneous high contrast materials and they have been used successfully in two-dimensional imaging applications when the properties of materials are not known at it is convenient to model the high contrast medium using the Kozlov's function $\exp S(x)/\epsilon$ ([24]) with a smooth phase function $S(x)$.

By contrast, we consider two phase dispersive composites (particles or fibers in a matrix) when the properties of each phase *are known* and the aspect ratio of materials parameters is taken to be *infinite*. The corresponding phase function $S(x)$ is just the non smooth characteristic function of the disks (is equal 1 on the disks and 0 otherwise) and the asymptotic parameter of our approximation is the *geometric* interparticle distance parameter.

As a result of the above mentioned differences, the fluxes in the discrete network in the Borcea-Kozlov-Papanicoalou model [9], [8] are described by the key parameter $\sqrt{k_+/k_-}$, where k_+ and k_- are the principal curvatures at the saddle point x of the function $S(x)$ where as in our model the fluxes in the network are described by the parameter $\sqrt{\frac{R}{\delta_{ij}}}$ (inverse of the root of the relative interparticle distance), where R is the radius of the inclusions (disks), δ_{ij} is the distance between the closely spaced neighbors (i-th and j-th disks). The parameter of the form $\sqrt{\frac{R}{\delta}}$, where δ is determined

by the volume fraction, appeared in the work [20] (see also [29]) where a periodic array of almost touching disks have been considered.

Thus we generalize and rigorously justified the Keller's type asymptotics for irregular (non periodic) high contrast composites. As a byproduct we also provide a framework for justification of the formal asymtotics which was developed in [20] for the periodic case.

Note that for the irregular (non periodic) geometry the interparticle distance parameter has qualitatively new features. Indeed, for a periodic array of inclusions (e.g. a quadratic lattice) the distance between all inclusions is the same that is $\delta_{ij} = \delta$ and the parameter δ/R is uniquely determined by the volume fraction of the inclusions. In a non periodic (random) medium with fixed volume fraction of the inclusions the parameter δ_{ij}/R *can vary*. So in an irregular (random) medium it is necessary to introduce an additional parameter δ/R, $\delta = max\delta_{ij}$. Here maximum is taken over all neighboring pairs, where the neighbors are defined using Voronoi tessellation. We call this parameter the"*relative interparticle distance*" and it describes the local geometry of the medium (as oppose to the volume fraction which is a "global" parameter. Parameters of a similar kind can be measured in an experimental setting and have been reported by experimentalists (see, for example [43]). In our work this parameter naturally appears as a result of a rigorous mathematical analysis.

In subsections 2.1-2.5 we construct trial functions for the direct and dual variational problems. Variational formulation of the problem with ideally conducting inclusions (conductivity is equal to infinity) requires introduction of a functional space different from usual H^1. Namely, we employ the space V_p of functions, which take (unknown) constant values on the inclusions (see section 5.1 for the precise definition). Similar spaces for an elastic problem with absolutely rigid inclusions were introduced in [5]. Therefore we must use a construction of trial functions different from [9]-[8], where the Kozlov's high contrast field of the form $e^{S(x)/\epsilon}$ was considered. In [9]-[8] the construction of trial functions was based on the solution of the ODE $(e^{S(x)/\epsilon}u')' = 0$. In our case$\epsilon = 0$ (infinite contrast), and since we consider a piecewise constant medium, we construct the trial functions in the neighborhood of each particle, assuming that they are constants on the particle. We remark here that the idea of construction of test functions for the direct and the dual variational problems have been used by several authors. However, there is no general recipe for constructing the test functions. For example, the test functions from [24] and [9]-[8] are different from ours and from each other due to different geometries.

Our construction of the trial functions employs the Keller's solution in a "neck" or channel between two neighboring disks and an extension in the rest of the domain. The construction of the extension is based on the partition of the domain due to Voronoi tessellation which is the key technical tool of this construction. We use the dual variational problem to obtain the lower bound for the effective conductivity $\hat{A}$. Main technical points here are to satisfy the *div*-free conditions and the balance of fluxes condition (see section 2.4).

In subsection 2.6 we formulate and prove the following asymptotic formula for the effective coefficient $\hat{A}$, which is the main mathematical result of our work.

$$\hat{A} = \frac{1}{4}\sum_{i,j=1}^{N} g_{ij}(t_i - t_j)^2 + F, \tag{0.1}$$

where t_i is a solution vector for the discrete network problem: $\sum_{i,j=1}^{N} g_{ij}(t_i - t_j) = 0$ for the interior sites of the network and $t_i = \pm 1$ for the sites on the upper and

lower boundaries of our rectangular domain (see Section II for precise definitions), $g_{ij} = \pi\sqrt{\frac{R}{\delta_{ij}}}$

The quantities $\hat{A}$ and $\sum_{i,j=1}^{N} g_{ij}(t_i - t_j)^2$ are of order $\sqrt{\frac{R}{\delta}}$, where $\delta = max\delta_{ij}$ and F is of the order $O(1) + \sqrt{\frac{R}{\delta}}O(\delta/R)$, $O(\delta/R) \to 0$ as $\delta/R \to 0$. So the leading term in the asymptotics in δ is of order $\sqrt{\frac{R}{\delta}}$ and it is explicitly calculated in terms of the vector solution of the discrete network problem. The condition $\delta \to 0$ means that we assume that the interparticle distances decay uniformly that is we have a uniformly dense packing of the particles. We introduce this assumption (which is quite physical) for the sake of simplicity. It is not too difficult to modify the proof for the case when the particles distribution consists of several densely packed clusters which are disconnected or when some isolated particles are present. Such modification can be done using the same network model. The condition of the uniformly dense packing is formalized in Section 2.6.

1. Mathematical model of a high contrast two-phase composite. The network approximation and numerical results. In this section we present a reduction of the continuum problem to a discrete network problem (approximation) using physical arguments. In Section II this approximation will be rigorously justified. Our main focus in this Section will be physical grounds for the network problem for the two-phase , composites and numerical results, which, in particular, show a very pronounced effect of polydispersity.

1.1. The Continuum Problem. General Description. In the introduction we presented several engineering problems which require calculation of the effective properties of two-phase composites of a matrix filled by a large number of inclusions (particles or fibers). The ratio between physical properties of the constituents in such composites (the contrast ratio) varies from several hundreds to several thousands. Then it is quite natural to ask whether one can assume that the inclusions are ideally conducting, i.e. having the dielectric constants or thermal conductivity or stiffness in the above examples formally set to be infinity. The answer to this question depends on the value of the contrast ratio. In general it is positive for the problems described in the introduction. For the value of the contrast ration, one can use, for example, Bruno bounds ([11], page 370). Then we arrive to a simplified model of finding the effective conductivity of a medium with randomly distributed absolutely conducting inclusions. From now on we will use the thermal conductivity language for the sake of definiteness. At the same time we emphasize that our model also applies to the electrostatic and mechanical problems.

Periodic arrays of high contrast inclusions have been studied in several works ([20], [5]). If the volume fraction is fixed then the parameter δ/R is uniquely determined. Here δ is the distance (spacing) between the neighboring inclusions , R is the size of the inclusion (e.g. the radius of a spherical inclusion). It was observed that for such periodic composites the effective conductivity is of order the conductivity of the matrix (see, for example, [3]),that is the filler has almost no effect The case of almost touching inclusions, when δ/R is small was considered in ([20], [29]). There the effective conductivity was found to be of order $\sqrt{R/\delta}$.

When the inclusions are randomly distributed, we can not use the techniques, based on the analysis of the periodic cell, which were used in [20], [29] for periodic

structures. Moreover for random structures the interparticle distance parameter δ is not uniquely determined by the volume fraction and should be viewed as an independent parameter and percolation effects (connectivity patterns) become very important. Note that our problems fall into the class of so-called continuum percolation problems ([33].

1.2. Mathematical Formulation of the Continuum Problem. The Discrete Approximation and physical grounds for its validity. We consider a two-dimensional model of a high contrast composite and assume that all inclusions are identical disks.

We next present three basic assumptions which were used in formulation of the discrete model. Note that in Section 1 we do not present rigorous justification of this model and rather use physical considerations.

- *On distribution of the inclusions.* All inclusions are modeled by circular disks D_i . The disks are uniformly distributed and do not overlap. The latter is achieved in the following way: if a randomly thrown in disk overlaps any other disc, which is already present, it does not count (i.e. it is disregarded).
- *On potentials on inclusions(disks).* The value of the potential ϕ on the disk is a constant, $\phi = t_i$ on D_i. The values t_i are unknown and have to be determined in the course of solving the problem.
- *On fluxes.* We take into account fluxes between the neighboring inclusions (i.e. closely spaced) only. All other fluxes (between disks, which are not closely spaced) and their influences on the nearest neighbors are neglected.

We next comment on these assumptions.

The first assumption is commonly used in modeling of randomly distributed particles and is known as a sequential addition procedure [33].

The second assumption corresponds to the so-called "stiff expansion" in the homogenization problem [3], and have been used for elastic media with rigid inclusions [5] and for thermal and electrical problems with "ideally conducting" inclusions.

The third assumption corresponds to the results obtained by J.B.Keller in [20] for fluxes in the high contrast periodic composite. In Section 2 this assumption will be rigorously justified for quite generic irregular (non periodic) geometries.

We now present rigorous mathematical model of a medium with a large number of "ideally conducting" inclusions (see the second assumption above). It is convenient to use the following variational formulation of the problem.

Introduce the domain $\Pi = [-L, L] \times [-1, 1]$ occupied by the composite, Fig.1.1. Denote the disks, which model the inclusions by D_i, i=1,...,N. N is the total number of the disks. Then $Q_p = \Pi \backslash \cup_{i=1}^{N} D_i$ is the matrix (the perforated domain). Introduce the functional space corresponding to the second assumption.

$$V_p = \{\phi \in H^1(Q_p) : \phi(\mathbf{x}) = t_i \text{ on } D_i, \phi(x, \pm 1) = \pm 1\} \tag{1.1}$$

The condition $\phi(x, \pm 1) = \pm 1$ corresponds to applying the potential ± 1 to the boundaries $y = \pm 1$ respectively.

Consider the following problem

$$I(\phi) = \frac{1}{2} \int_{Q_p} |\nabla \phi|^2 d\mathbf{x} \to min \ , \ \phi \in V_p \tag{1.2}$$

The problem (1.1)- (1.2) is equivalent to the following boundary value problem:

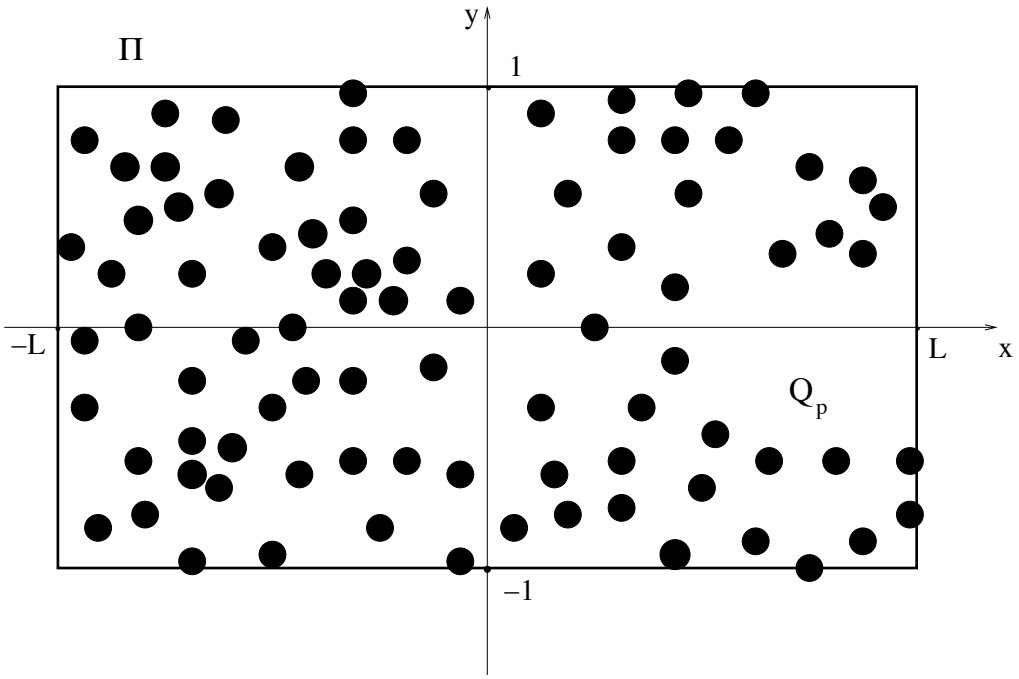

FIG. 1.1. *The composite*

$$\Delta\phi = 0 \text{ in } Q_p \tag{1.3}$$

$$\phi(\mathbf{x}) = t_i \text{ on } \partial D_i \tag{1.4}$$

$$\int_{\partial D_i} \partial\phi/\partial\mathbf{n} d\mathbf{x} = 0 \tag{1.5}$$

$$\phi(x, \pm 1) = \pm 1 \tag{1.6}$$

$$\partial\phi/\partial\mathbf{n}(\pm L, y) = 0 \tag{1.7}$$

Here and below $x = \pm L$ means the vertical (left and right) boundaries of the domain Q_p, $y = \pm 1$ means the horizontal boundaries of the domain Q_p.

Condition (1.5) is obtained by integration by parts in the Euler-Lagrange equation, which corresponds to the functional(1.2) and by taking into account condition (1.4). Condition (1.7) means the absence of the flux through the vertical boundaries of the domain Π.

*Formulas for the effective conductivity.*The effective conductivity from the physical point of view is defined as the total flux through a cross-section of the domain, for example, through the upper boundary $y = \pm 1$. We will need the expression for this flux in terms of the value of the energy integral $I(\phi)$, which is commonly used in the homogenization theory as a definition of the effective coefficient [4]. For the sake of completeness we present here this simple derivation.

Multiply equation (1.3) by ϕ and integrate by parts. Then we obtain

$$0 = -\int_{Q_p} |\nabla\phi|^2 \delta\mathbf{x} + \int_{y=\pm 1} \partial\phi/\partial\mathbf{n}\phi\delta\mathbf{x} + \sum_{i=1}^{N} \int_{\partial D_i} \partial\phi/\partial\mathbf{n}\phi\delta\mathbf{x} \tag{1.8}$$

Then for the integrals over the boundaries we use (1.4)-(1.5) and obtain

$$\int_{\partial D_i} \partial\phi/\partial\mathbf{n}\phi d\mathbf{x} = t_i \int_{\partial D_i} \partial\phi/\partial\mathbf{n} d\mathbf{x}. \tag{1.9}$$

Furthermore,

$$\int_{y=\pm 1} \partial\phi/\partial\mathbf{n}\phi d\mathbf{x} = \int_{y=1} \partial\phi/\partial\mathbf{n} d\mathbf{x} - \int_{y=-1} \partial\phi/\partial\mathbf{n} d\mathbf{x} \tag{1.10}$$

due to (1.6).

Multiply the equation (1.3) by 1 and integrate the result by parts. We obtain

$$0 = \int_{y=\pm 1} \partial\phi/\partial\mathbf{n}1 d\mathbf{x} + \sum_{i=1}^{N} \int_{\partial D_i} \partial\phi/\partial\mathbf{n}1 d\mathbf{x}$$

The last integral is equal to zero due to (1.5) . Then

$$\int_{y=1} \partial\phi/\partial\mathbf{n} d\mathbf{x} + \int_{y=-1} \partial\phi/\partial\mathbf{n} d\mathbf{x} = 0$$

From the last equality and (1.10) we get

$$\int_{y=\pm 1} \partial\phi/\partial\mathbf{n}\phi d\mathbf{x} = 2\int_{y=1} \partial\phi/\partial\mathbf{n} d\mathbf{x} \tag{1.11}$$

Combining (1.8), (1.9) and (1.11) we obtain

$$\int_{y=1} \partial\phi/\partial\mathbf{n} d\mathbf{x} = \frac{1}{2}\int_{Q_p} |\nabla\phi|^2 d\mathbf{x}, \tag{1.12}$$

where ϕ is the solution of the problem (1.3)-(1.7) ((1.1)-(1.2)).

DEFINITION 1.1. *The total flux through the boundary $y = 1$ per unit length defined by*

$$\hat{a} = \frac{1}{2L} \int_{y=1} \partial\phi/\partial \boldsymbol{n}\, d\boldsymbol{x}.$$

is called the effective conductivity*.*

We shall also use the corresponding normalized quantity $\hat{a}$ defined by $\hat{A} = 2\hat{a}L = \int_{y=1} \partial\phi/\partial \mathbf{n}\, d\mathbf{x}$.

Due to (1.12) we have the following formulas for $\hat{A}$

$$\hat{A} = \frac{1}{2} \int_{Q_p} |\nabla\phi|^2 d\mathbf{x} \tag{1.13}$$

$$\hat{A} = \int_{y=1} \partial\phi/\partial \mathbf{n} d\mathbf{x}, \tag{1.14}$$

where ϕ is solution of the problem (1.3)-(1.7)or due to (1.2),

$$\hat{A} = \frac{1}{2} min_{\phi \in V_p} \int_{Q_p} |\nabla\phi|^2 d\mathbf{x} \tag{1.15}$$

We remark here that the conductivity of the matrix is taken to be 1 therefore the flux in the matrix is given by $\nabla\phi$.

The discrete problem. We have expressed $\hat{A}$ in terms of the flux which allows us to use the third assumption (Sect1.2) in order to calculate the effective coefficient$\hat{A}$. According to this assumption, we take into account only the fluxes in the "necks"(channels) connecting the neighboring disks and neglect all other fluxes. The we need to know the flux between two disks if the potential on each disk is a constant. A simple approximate formula for this flux was obtained in [20] (for identical disks). We employ Keller's method to derive an approximate formula for the flux between two disks (the i-th and the j-th) of arbitrary radii R_i and R_j, (see Fig.1.2). Following [20], we approximate the disks by the tangential parabolas

$$y = -(\delta/2 + \rho_i x^2/2)$$

and

$$y = \delta/2 + \rho_j x^2/2,$$

where

$$\rho_i = 1/R_i, \rho_j = 1/R_j$$

The distance between the parabolas is equal to

$$H(x) = \delta + (\rho_i + \rho_j)x^2/2, \tag{1.16}$$

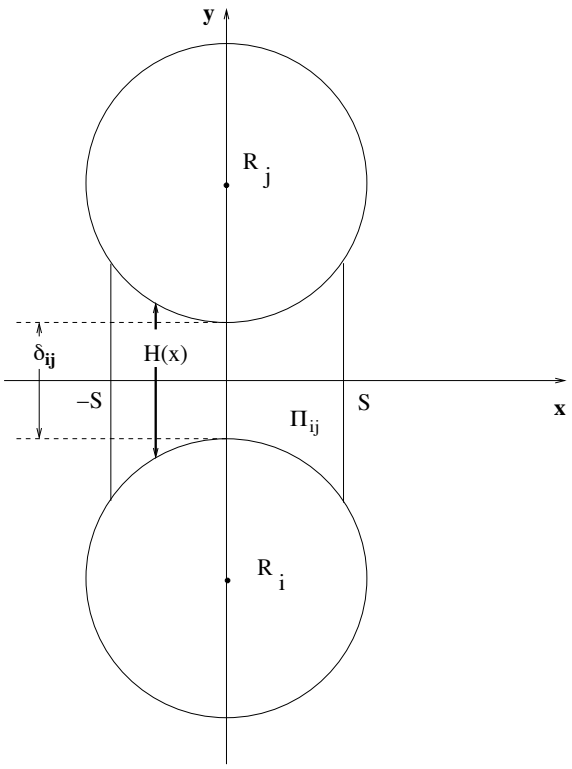

FIG. 1.2. *Keller's solution for two disks*

We assume that the local flux (the gradient of the potential) between the disks is of the form

$$(0, \frac{t_i - t_j}{H(x)}), \tag{1.17}$$

that is we assume that it is proportional to the difference in temperature or potential and inversely proportional to the distance between the disks.

Then the total (integral) flux between the disks can be calculated as follows:

$$J_{ij} = (t_i - t_j) \int_{-S}^{S} \frac{dx}{\delta + (\rho_i + \rho_j)x^2/2} = \frac{1}{((\rho_i + \rho_j)/2)^{1/2}\delta^{1/2}} tan^{-1}[(\frac{(\rho_i + \rho_j)/2}{\delta})^{1/2} x]|_{-S}^{S} \tag{1.18}$$

If the sum of the curvatures $\rho_i + \rho_j$ is not small, and the distance δ between the disks is small, then the value of tan^{-1} in the right-hand side (1.18) is approximately π. Taking into account that $\rho_i = 1/R_i, \rho_j = 1/R_j$ we obtain

$$J_{ij} = (t_i - t_j) g_{ij}, \text{where } g_{ij} = \frac{\pi \sqrt{\frac{2R_i R_j}{R_i + R_j}}}{\sqrt{\delta}} \tag{1.19}$$

Note that g_{ij} is the specific flux (i.e. per unit difference of potential).

Formula (1.19) can be derived from the exact solution of the Laplace equation for two disks as the leading term in asymptotics in δ. This exact solution (capacity of two cylinders) can be found in [37].

We now estimate the characteristic values of the flux for the different characteristic distances between the disks. Introduce the following two characteristic distances between a given inclusion and all other inclusions:

- Distance between the nearest neighbors (closely spaced) inclusions (see also Fig. 1.2). Denote it by δ^* (order of magnitude). Then $\delta^* << R$ for very close packing (see Section 2 for rigorous definitions).
- The distance between a given inclusion and inclusions which are not close to it (non neighboring). These inclusions form so to speak "second belt" and the corresponding distances are greater than δ^*. For the sake of definiteness we choose this second order distance to be of order R.

We comment here on the choice of the cut-off distance δ^* in numerical simulations. We used visual control that is many randomly generated pictures were examined. We considered neighbors the disks, which share common edge in the Voronoi tessellation (see Section 2.3 for the precise definition). The neighbors in a random array of the disks are not necessarily closely spaced. The heuristic idea behind our approach is that we take into account the fluxes between the closely spaced inclusions only. To make the latter more precise we choose the cut-off distance δ^* in the interval $0.3R - 0.5R$ and obtain a connected graph (network), which consists of the center of closely spaced disks. The graph is a discrete object. It is controlled by the continuous real variable δ^* and it changes by "jumps" as δ^* changes. The choice of the interval $0.3R - 0.5R$ is motivated by the fact that numerical simulations show that even if the disks are not quite of identical sizes, but the variability in the sizes is not large (factor 2 or 3), then we obtain stable, consistent pictures, that is all closely spaced neighbors are connected and the disks which are not closely spaced neighbors are not connected. We have also used another numerical criterion to support this choice of the cut-off distanceδ^*. Namely, if δ^* is increased, then the effective conductivity practically does not change.

The characteristic values of the fluxes corresponding to these distances are given by

$$J(distance = \delta^*) \sim \sqrt{\frac{R}{\delta^*}},\ J(distance = R) \sim 1$$

The first value is obtained from (1.19). The second value can be obtained from [37] and it is also consistent with (1.19).

Then, we get

$$\frac{J(distance = \delta^*)}{J(distance = R)} \sim \sqrt{\frac{R}{\delta^*}}$$

Thus, by assumption 3 (see the beginning of this subsection), we have to neglect the fluxes of order 1 and keep the fluxes of order $\sqrt{\frac{R}{\delta^*}}$, where R is the characteristic radius of the inclusions and δ^* is the characteristic distance between the inclusions.

1.3. Numerical implementation of the discrete network approximation and fluxes in the network. We now define the discrete network, which corresponds to the original continuum model and formulate the discrete problem.

By assumption 1 (on distribution of the inclusions, see Sect. 1.2) we create numerically a distribution of disks for a given radius (radii for polydispersed case) in the rectangle $\Pi = [-L, L] \times [-1, 1]$. The center $\mathbf{x}$ of each disk is generated as a uniformly distributed in Π random variable. If a disk with the center $\mathbf{x}$ and radius R overlaps with any disk which is already present, then it is rejected, otherwise it is accepted and added to the list of the disks

$$L = \{(\mathbf{x}_i, R), i = 1, ..., N\} \tag{1.20}$$

We stop throwing in the disks when the prescribed volume fraction of the disks

$$V = \sum_{i=1}^{N} \pi R^2 / (\text{square of } \Pi)$$

is achieved. Here N is the total number of the disks. We remark here that this procedure works well for relatively small radii of the disks, when the the fraction of the boundary disks is not too high.

We compute the distances δ_{ij} between the i-th and the j-th disks for the obtained distribution of disks. Then we determine the flux between the neighboring disks and neglect the fluxes between the non neighboring disks. For this purpose we introduce the following set of numbers:

$$g_{ij} = \begin{cases} g_{ij} & \text{calculated with formula (1.19)} \quad \text{if } \delta \le \delta^* \\ 0 & \text{if } \delta \ge \delta^*. \end{cases} \tag{1.21}$$

The quantity g_{ij} defined by (1.21) describes the flux between the i-th and the j-th disks. Thus we have defined a discrete network model (graph),

$$N = \{\mathbf{x}_i, g_{ij}; i, j = 1, ..., N\}, \tag{1.22}$$

which consists of points or sites x_i (centers of the disks) and edges with assigned numbers g_{ij}. The discrete model (1.22) does not explicitly contain the sizes of the disks and the distances between them, this information is incorporated via the set g_{ij}. Note that if the concentration is small g_{ij}, which gives zero value of the effective conductivity whereas the conductivity of the matrix is 1. This is not a contradiction. It means that for high contrasts the value 1 becomes negligible.

The fluxes g_{ij} are concentrated in the necks between the disks. Any given pair of disks is connected by a unique neck. For the disks which are close to the boundaries $y = \pm 1$ this is no longer the case, since a neck between the boundary and a disk which lies close to this boundary is not well defined. To avoid this difficulty, we introduce the notion of a "quasidisk"

Definition 1.2. *Consider a disk, which lies near the boundary $y = +1$, that is if we project this disk on the boundary $y = +1$ parallel to the OY-axis, then the projecting rays do not cross any other disk (see Fig.1.3). We call this projection a "quasidisk".*

In the section II we will provide another (equivalent) definition of quasidisks using Voronoi tessellation.

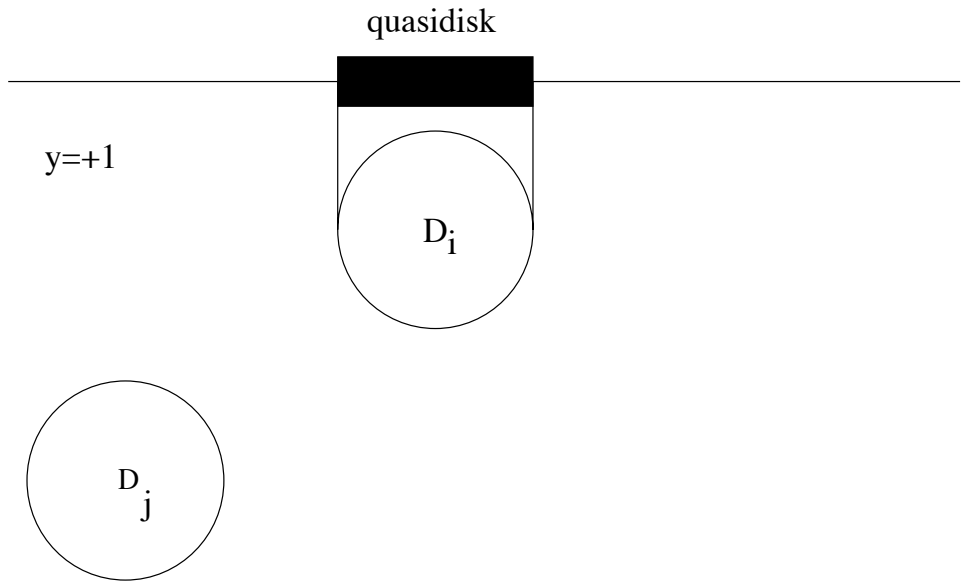

FIG. 1.3. *A quasidisk*

Same definition works for the boundary $y = -1$. In other words a quasidisk is an "image" of a disk which lies close to the boundary and it represents interaction between this disk and the boundary. Note that in our further consideration we will not distinguish the disks and quasidisks, which is a very convenient way to incorporate the boundary effects. Also when fluxes are computed one can treat any quasidisk as a disk of infinite radius ($R = \infty$) (or zero curvature).

We now present the motivation for our choice of the cut-off distance δ^*. If one looks at the pictures obtained as a result of the numerical procedure for placing random disks on the plane it is easy to see that with respect to each given disk all other disks fall into one of the two categories: closely spaced neighbors (or simply *"neighbors"*) and remote disks("aliens"). More precisely, a typical disk has 5-6 " neighbors", the distance between the given disk and its neighbors can be small ($\delta_{ij} \ll R$), whereas the distance between the given disks and the "aliens" can not be small(at least of order of R). The "neighbors", which can be in a close contact with form given disk form some sort of a belt which separates the given disk from the rest ("aliens"). The fluxes between non neighbors are negligible and the network approximation ignores them. We introduce the cut-off distance $\delta^* = R$ based on the analysis of the arrays obtained numerically in the procedure described above.

In Section 2 we justify the network approximation the δ close packing condition and present mathematical conditions for its validity the (the δ close packing condition).

To close up this model we need to obtain equations, which determine the (constant) values t_i of the potential on the sites x_i of the network (1.22). To this end we we note that by assumption 3 (see beginning of Sect. 1.2), only fluxes between nearest neighbors contribute into the integral (1.2). The latter contributions are given by (1.19). Using (1.21), we see that a discrete version of the Dirichlet energy integral

(1.2) for our network model has the following form

$$\frac{1}{4}\sum_{i,j=1}^{N} g_{ij}(t_i - t_j)^2,$$

where the factor $\frac{1}{4}$ appears due to the fact that we count each neck twice (see also a more detailed explanation right before 2.36).Thus we obtain a discrete minimization problem

$$\sum_{i,j=1}^{N} g_{ij}(t_i - t_j)^2 \to min, \tag{1.23}$$

which corresponds to (1.2). It remains to supply (1.23) with the boundary conditions

$$t_i = \pm 1 \text{ for } i \in S^{\pm} \tag{1.24}$$

Hereafter we use the notation $S^{\pm}$ for the set of disks, which touch, cross or lye on (if quasidisks) the boundaries $y = \pm 1$ respectively (boundary sites). The rest of the sites denoted by $I = \{x_i, i = 1, ..., N\} \setminus (S^+ \cup S^-)$ we are called the internal sites of the network.

Then the minimization problem (1.23) amounts to an algebraic system (of Kirchhoff's type)

$$\sum_{j=1}^{N} g_{ij}(t_i - t_j) = 0,\ i \in I \tag{1.25}$$

Finally we write a discrete formula for the effective conductivity which corresponds to (1.14):

$$\hat{A} = \sum_{i \in S^+} \sum_{j \in I} g_{ij}(1 - t_j) = 0,\ i \in I \tag{1.26}$$

($t_i = 1$ when $i \in S^+$).

LEMMA 1.3 (Discrete maximum principle). *Solution of the problem (1.24), (1.25) satisfies the inequalities* $-1 \le t_i \le 1$ *for all* $i = 1, ..., N$.

Proof. From (1.25) we have the following analog of the mean value theorem.

$$t_i \sum g_{ij} = \sum g_{ij} t_j, i \in I \tag{1.27}$$

where summation is taken over all adjacent sites (i.e. connected by an edge of our graph or network to the i-th site). We make use of the fact that the equality (1.27) holds on the boundary $x = \pm L$. From the formula (1.27) it follows that the maximum value cannot be achieved in a inner site. We prove this by contradiction. Suppose that the maximum value M is achieve at some inner site $i \in I$. Then $t_j = M$ at all sites adjacent to the i-th site. Otherwise (1.27) implies $M < M$. Since our graph is

connected it follows that $t_j = M$ for all sites of the graph. But the graph includes the sites on the upper and lower boundaries S^+ and S^-, where $t_j = 1$ and $t_j = -1$ respectively. This leads us to a contradiction, which means that the maximum value can be achieved only at the boundaries and this maximum value is 1.

The same argument works for the minimum value -1.

The proposition provides an analog of the maximum principle and it provides an estimate on the solution which does not depend on the coefficients g_{ij}. This lemma will be used in Section II, when constructing the test functions inside the triangles (see Fig. 2.4). For the sake of completeness we also mention that an alternative proof can be obtained by the following variational argument. The set $\{t_i\}$ solves the energy minimization problem(1.23). If $t_k > 1$ for some inner site k, then the energy can be lowered by choosing $t_k = 1$ and we are still in the admissible class since this procedure does not change the boundary conditions. The same argument works for $t_k < -1$ in which case we choose the replacement value to be -1.

1.4. Numerical simulations. We have implemented a numerical method to

- Generate a configuration ω as a system of random disks (according to assumption 1 at the beginning of section. 1.2)
- Compute the coefficients g_{ij} for this system of disks.
- Solve the linear system (1.24),(1.25).
- Compute the effective conductivity $\hat{A}(\omega)$ using formula (1.26) for this configuration.

The control parameters are: the diameter of the disks R and the total volume fraction V of the disks.

In order to collect the statistical information, we run the program repeatedly and collect the data $\{\hat{A}(\omega), \omega \in \Omega\}$. Then we compute

- The expected value of the effective conductivity $\hat{A} = E\hat{A}(\omega)$
- The mean deviation $DA = E|\hat{A}(\omega) - \hat{A}|$.
- The maximal conductivity over all collected data $m = max_{\omega\in\Omega}\hat{A}(\omega)$.

All the above quantities have been computed for given values of the quantities R and V which is why $\hat{A}, DA, m = \hat{A}, DA, m(R, V)$ are functions of R and V.

Numerical results for monodispersed composites (all disks of the same radius). The goal here is to test our numerical algorithms which are based on the network approximation, to make sure that we can consistently recover (in a very efficient way) known results, in particular, recover the percolation picture.

The simulations have been carried out in the following way. All disks were of the same radius. The volume fraction V has been increased with a fixed step δV.For each value of V the effective conductivity $\hat{A}(\omega)$ have been computed using the above described procedure.

For each fixed V the quantities $\hat{A}, DA$ and $m(\omega)$ have been computed repeatedly for different random configurations ($100 - 300$ configurations for each value of V).

We have used several sets of identical disks, that is three different disks' sizes (15, 20 and 25) have been used to control the stability of our numerics. Indeed, since the problem is scale invariant the choice of the radius should not change the effective conductivity. This effect was used for checking the numerical process. We have observed no difference in qualitative and quantitative dependence of $\hat{A}$ on the volume fraction V when the sizes were changed.

A typical plot of the function $\hat{A} = \hat{A}(\omega)$ is shown at Fig.1.4. The plot consists of two parts: for $V \leq 0.2$; the total flux through the composite layer is zero. More precisely, it is very small and it is very close to the OX axis at the plot. For $V \geq 0.35$

the total flux is for sure positive (taking into account the mean deviation). In the range $V = 0.2 - 0.35$ the total flux is not positive for sure. Thus the plots of the function $\hat{A} = \hat{A}(V)$ reveal dependence which is typical in the percolation processes [38]. The percolation threshold in all computations can be estimated as $V_0 \approx 0.24$. Above the threshold the function $\hat{A}(V)$ behaves as $const(V - V_0)^p$ with $p \geq 1$, which is consistent with conventional percolation picture which was observed in experiments and explained by the percolation theory scaling arguments. We have done this plot

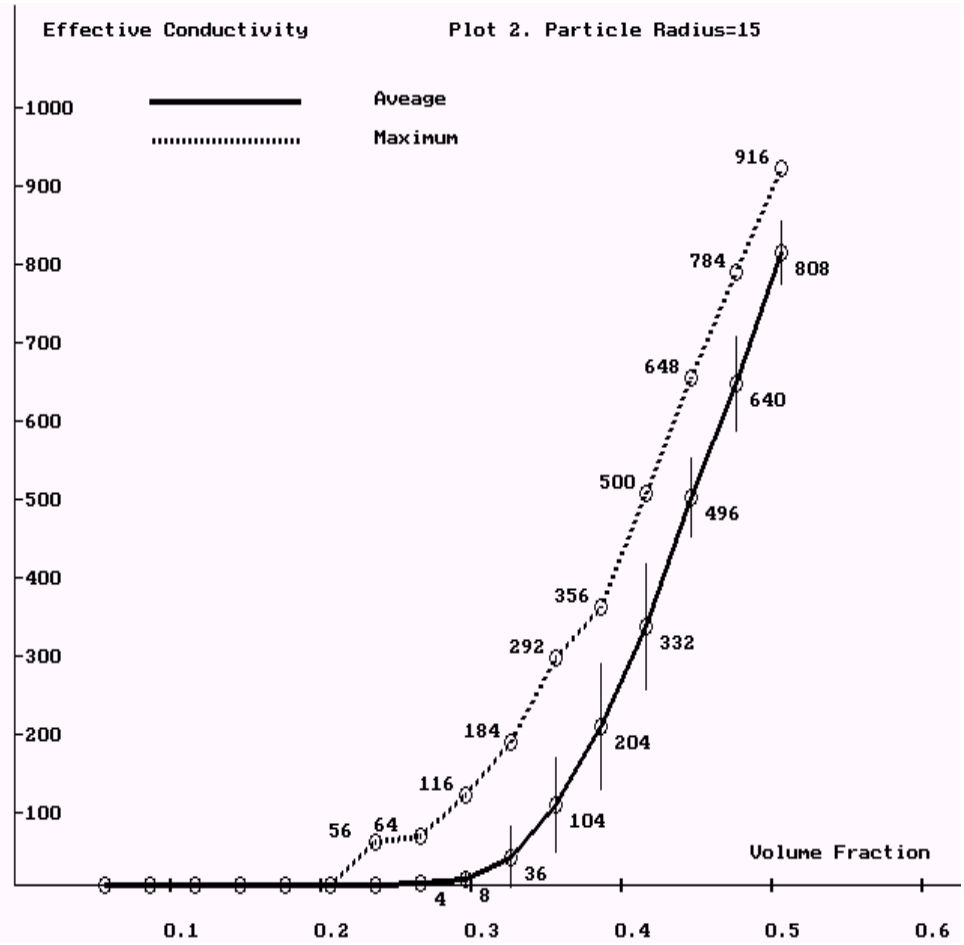

FIG. 1.4. *The monodispersed composite*

for several sizes of identical inclusions to make sure that there is no size effect, which is in principle can appear as a numerical artifact.

Thus we conclude that our numerical analysis captures basic features of the real physical phenomenon and provides realistic quantitative predictions.

We have used the graph of the maximal value $m(\omega)$ as an additional test for our code. Indeed, from the physical point of view it should behave (qualitatively) in the same way as the graph for the average conductivity, which is what one can see at Fig.1.4.

The polydispersed composite. We call a composite polydispersed, if it is filled with inclusions of different sizes. In our model it amounts to consideration of disks of different radii. The distribution of the sizes can be continuous or discrete. We consider the discrete case that is we consider the disks of several fixed sizes. For the sake of simplicity we study the bimodal case. Namely we have analyzed the following two components mixtures:

MIXTURE 1. The radii of the disks are: $R_1 = 25, R_2 = 15$; the relative fractions are $V_1 = 33\%, V_2 = 67\%$ respectively

MIXTURE 2. The radii of the disks are: $R_1 = 25, R_2 = 15$; the relative fractions are: $V_1 = 67\%, V_2 = 33\%$ respectively.

MIXTURE 3. The radii of the disks are: $R_1 = 35, R_2 = 15$; the relative fractions are $V_1 = 34\%, V_2 = 66\%$

MIXTURE 4. The radii of the disks are: $R_1 = 35, R_2 = 15$; the relative fractions are $V_1 = 66\%, V_2 = 34\%$

The total volume fraction of the disks varies in the interval $[0.4; 0.55]$. The total volume fraction 0.55 is practically the maximal volume fraction which can be achieved in our procedure (see Assumption 1 on non overlapping). We used the following two step procedure for generating the polydisprsed (bimodal) random configurations of the disks. First we used the algorithm described in Assumption 1 at the beginning of Sect. 1.2) for the disks of larger size until we reach the volume fraction $V \times V_1$. Next we use the same algorithm for the small disks with the volume fraction $V \times V_2$, where V is the total volume fraction of disks (kept fixed). In the second step we take into account the large discs generated in the first step that is if a small disk overlaps with any other disk present (small or large) it is rejected. The cut-off distance for both steps is $0.3R_2 - 0.5R_2$.

The graphs of the effective constant $\hat{A}$ as a function of the total volume fraction V are presented on Fig.1.5

One can see that the plots, which correspond to MIXTURES 1-3, are very similar. It means that in these cases we observe no influence of polydispersity on the effective constant.

At the same time the graph which corresponds to MIXTURE 4 differs from the others. This leads us to assume that the polydispersity may or may not have an essential influence on the effective conductivity, depending on the relative volume fractions of the large and the small inclusions. Note that MIXTURE 4 has a large relative volume fraction.

By the latter observation we decided to study the influence of polydispersity in more detail. For this purpose we have studied the following mixture.

Radii of the disks: $R_1 = 25, R_2 = 10$; the total volume fraction of the disks V is equal to 0.55. We vary the relative volume fraction of the inclusions V_1 and V_2 ($V_1 + V_2 = 1$) from0 to 1. In the Plot 3 the effective conductivity is presented as function of V_1, which is the relative volume fraction of the disks of radius $R_1 = 25$.

This graph shows the same values of $\hat{A}$ for $v_1 = 0$ and $v_1 = 1$ (that is no size effect, which agrees with the theory, since the problem is scale invariant) and it *plunges down sharply* in the interval $[0.5; 0.9]$. The latter agrees with the above result for MIXTURE 4.

Thus we observe that for this mixture polydispersity can decrease the effective conductivity by approximately a factor of 2. This sharp drop occurs when the relative volume fraction v_1 of the large particles is quite high. If we compare the minimum value $\hat{A}(v_1 = 0.9) = 484$ with the corresponding value in a monodispersed composite:

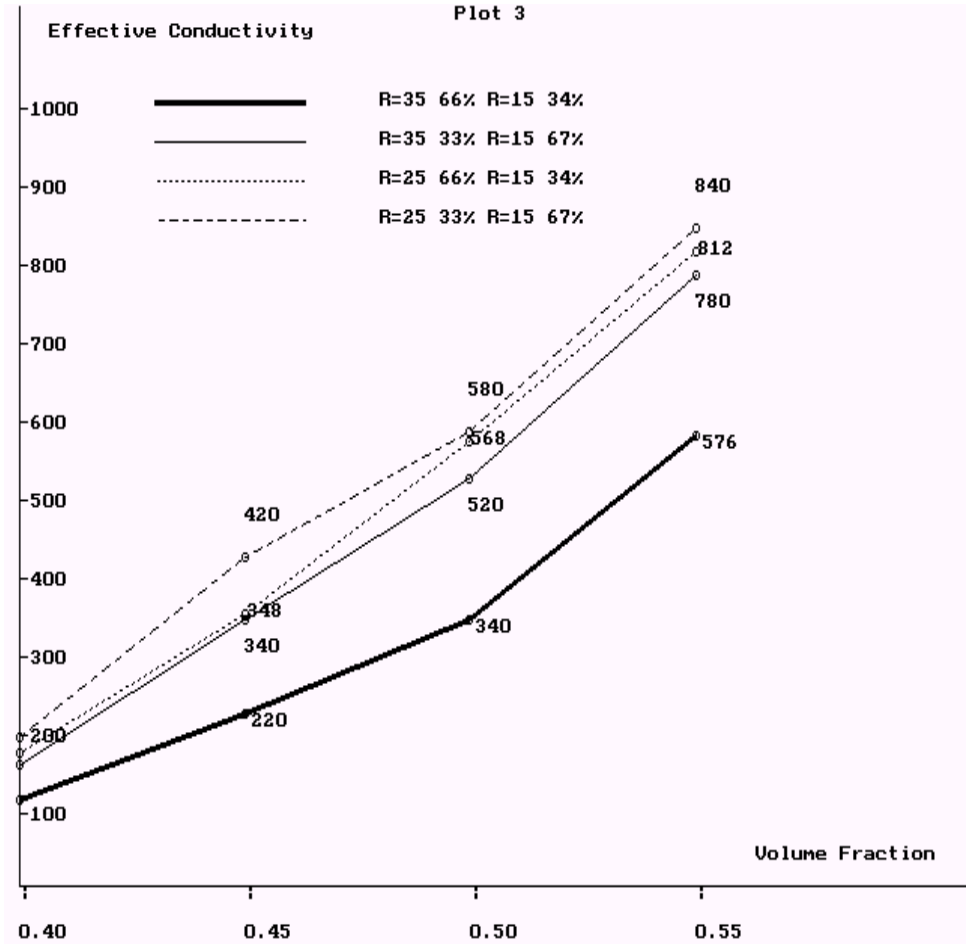

FIG. 1.5. *The polydispersed composites*

$\hat{A}(0.9V \approx 0.5) = 680$, then we conclude that the small particles practically do not contribute into the effective conductivity.

Note that the effect of polydispersity have been considered in [40] for the dilute limit and in [41] for a non dilute case (but far from close touching and for a periodic structure). What concerns us here is the random close packing case (almost touching). In [40] polydispersity implies a slight increase in the effective conductivity and in [41] a heuristic and numerical analysis predict that the effect of polydispersity is very small. In the almost touching case we observe either very small effect or essential drop in the effective conductivity.

We remark here on the comparison of the results in the dilute limit (where in essence only pairwise interactions are taken into account), the fixed concentration case (which reduces to a cell problem in the periodic case) and almost touching random packing (our case) suggests that the effect of polydispersity manifests itself differently for three qualitatively different ranges of the fillers concentration (dilute irregular, periodic finite concentration and almost touching irregular).

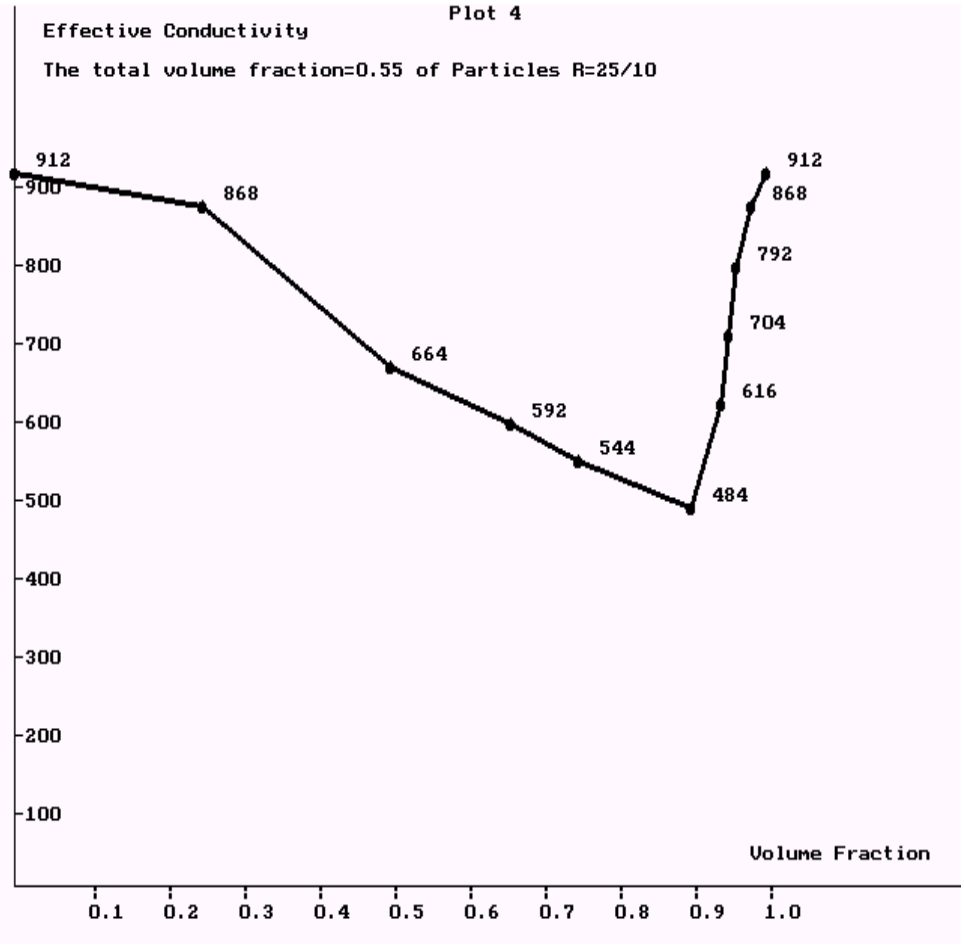

FIG. 1.6. *Sharp decrease in the effective conductivity*

Description of the numerical procedure. In our numerical simulations we have used an integer lattice $\Pi_0 = 550 \times 400$, i.e. we have chosen the rectangle $\Pi_0 = [0, 550] \times [0, 400]$ (that is $L = 550/400$ for convenience of the visual control on the screen). The centers of the disks have been generated in the form $random(n) + random(1)$, where $random(n)$ is a pseudo-random number uniformly generated from the set $\{0, 1, ...n\}$ and $random(1)$ is is a pseudo-random number uniformly generated from the interval $[0, 1]$. The disks near the boundary were retained if their centers were inside Π_0. The boundary values 1 and 0 were prescribed at the upper and lower edges of Π_0.

In the numerical procedure we have used the disks of radii $35, 25, 20, 15, 10$ (in our coordinates $35/200, 25/200, 20/200, 15/200, 10/200$, since $[-1, 1]$ corresponds to $[0, 400]$ and there were from 5 to 20 layers of disks on the top of each other in the vertical direction. The statistical data was collected mainly for the disks of radii $25, 20, 15$. The average number of disks in the rectangle Π_0 was between 50 and 150.

In the numerical experiments for the monodispersed composites the expected value of $\hat{A}$‘ and the deviation $D\hat{A}$ was calculated over 320 configurations for several

values of the volume fraction V, which are indicated at the plots as nodal points. The values of $\hat{A}$ at these points are also indicated at the plots. The vertical segments at the plots corresponds to the intervals $2[E\hat{A} - D\hat{A}]$. We observe that the graphs, which corresponds to different volume fractions are similar both qualitatively and quantitatively. Also one can see that $m(V)$ and $E\hat{A}(V)$ have the same qualitative behavior. Thus we conclude that our numerical procedure is stable.

We now introduce the interparticle distance parameter, which will be used in the justification of the asymptotic formula.

To this end we first recall the notion of the two-dimensional Voronoi tessellation. It illustrated by Fig. 1, where the boundaries of the polygons are formed from the points which are equidistant from the given set of sites x_i. Thus the Voronoi polygon (more precisely its interior) of the site x_i is the set of all points which are closer to the site x_i than to any other site $x_j,\ j \neq i$. This definition works for the set of points (sites) of an infinite plain.

It also can be adopted for a set of points (sites) inside our rectangular domain Π. It could be done in a number of ways, for example, by the symmetric reflecting of the domain Π and set of sites x_i about each edge of Π followed by restriction of the Voronoi cells in the broader domain ("4Π") to the original domain Π.

In the context of our problem we shall do the following. Given a set of randomly distributed disks in the domain Π, we take the centers x_i as the sites of the Voronoi tessellation of Π. Then the neighboring Voronoi polygons (cells) determine the neighboring disks (neighboring cells shear a common edge).We connect the neighborings sites x_i and x_j by segments $x_i\ x_j$. We then connect the sites near the boundary of Π (centers of the disks which lie near the boundary) with the boundary by perpendiculars from this centers to the corresponding (nearest) edges of Π. Here we have treated pieces of the boundaries as quasidisks.

2. Approximation of the continuum problem by the discrete problem. Estimates and proof of convergence.

2.1. Direct problem. In Section 1 we introduced the affine set of functions

$$V_p = \{\phi \in H^1(Q_p) : \phi(\mathbf{x}) = t_i \text{ on } D_i, \phi(x, \pm 1) = \pm 1\} \tag{2.1}$$

It consists of the functions which take constant values on the inclusions D_i $i = 1, ..., N$ (N is the total number of the inclusions) and satisfy the boundary conditions on the vertical boundaries $y = \pm 1$ of the domain Q_p (see Fig.1.1, Section 1).

We have also shown that the problem under consideration can be written in variational form (minimization of a functional) and as a boundary value problem. For our purposes we will use the following variational form (see Section 1 (1.2)):

$$I(\phi) = \frac{1}{2}\int_{Q_p} |\nabla\phi|^2 d\mathbf{x} \to min\ ,\ \phi \in V_p \tag{2.2}$$

It has been also shown that (see (1.13)) that the integral flux $\hat{A}$ through the boundary y=+1 of the domain Q_p is equal to

$$\hat{A} = \frac{1}{2}\int_{Q_p} |\nabla\phi|^2 d\mathbf{x}, \tag{2.3}$$

where ϕ is the solution of the problem (2.2) and therefore

$$\hat{A} = \frac{1}{2} min_{\phi \in V_p} \int_{Q_p} |\nabla \phi|^2 d\mathbf{x}, \tag{2.4}$$

The quantity $\hat{A}$ is a rescaled effective conductivity $\hat{a}$ so that $\hat{A} = 2\hat{a}L$. In order to get rid of the normalization factor L we will deal with $\hat{A}$.

From (2.4) and (2.2) we have an upper bound

$$\hat{A} \leq \frac{1}{2} \int_{Q_p} |\nabla \phi|^2 d\mathbf{x} \text{ for any } \phi \in V_p \tag{2.5}$$

2.2. The dual problem. The dual problem can be introduced in a standard way. Some specific features are due to the fact that the trial functions take constant values on the inclusions.

Let us introduce the following functional space

$$W_p = \{\mathbf{v} \in L_2(Q_p) : \mathbf{v}(\pm L, y)\mathbf{n} = 0; \int_{\partial D_i} \mathbf{v}\mathbf{n} d\mathbf{x} = 0\} \tag{2.6}$$

Here $\mathbf{vn}$ is the dot product, the condition $\mathbf{v}(\pm 1, y)\mathbf{n}$=0, where $\mathbf{n}$ is the outward normal to the vertical boundaries of the domain Q_p corresponds to insulating boundaries (see (1.7)). The second (integral) condition in (2.6) will be explained later.

We next use the Legendre transformation

$$\frac{1}{2}\mathbf{x}^2 = max_{\mathbf{v} \in R^2}(\mathbf{v}\mathbf{x} - \frac{1}{2}\mathbf{v}^2), \mathbf{x} \in R^2 \tag{2.7}$$

Then (2.4) can be written in the form

$$\hat{A} = min_{\phi \in V_p} \int_{Q_p} \frac{1}{2} |\nabla \phi|^2 d\mathbf{x} = min_{\phi \in V_p} max_{\mathbf{v} \in W_p} \int_{Q_p} (\nabla \phi \mathbf{v} - \frac{1}{2}\mathbf{v}^2) d\mathbf{x} =$$
$$max_{\mathbf{v} \in W_p} min_{\phi \in V_p} \int_{Q_p} (\nabla \phi \mathbf{v} - \frac{1}{2}\mathbf{v}^2) d\mathbf{x} \tag{2.8}$$

We will use the weak formulation of the divergence-free condition and the weak formulation of the boundary conditions for the trial fields $\mathbf{v}$.

Since the quadratic functional $I(\phi)$ satisfies the conditions of Proposition 5.2, Chapter III [14], we can interchange max and min in (2.8). Here the div free condition is understood in the weak sense (see (2.11) below).

Since the term $\frac{1}{2}\mathbf{v}^2$ in (2.8) does not contain ϕ, it is possible write (2.8) in the form

$$\hat{A} = max_{\mathbf{v} \in W_p} \{ \int_{Q_p} -\frac{1}{2}\mathbf{v}^2 d\mathbf{x} + min_{\phi \in V_p} \int_{Q_p} \nabla \phi \mathbf{v} d\mathbf{x} \}$$

We integrate by parts in the last integral taking into account that the boundary of the domain Q_p consists of the external boundaries of the rectangle $x = \pm L, y = \pm 1$, see Fig.1.1, Section 1) and boundaries ∂D_i of the inclusions D_i (i=1,...,N).

Then we get

$$\hat{A} = max_{\mathbf{v}\in W_p}\{\int_{Q_p} -\frac{1}{2}\mathbf{v}^2 d\mathbf{x} + min_{\phi\in V_p}[-\int_{Q_p}(\phi div\mathbf{v}d\mathbf{x} + \int_{x=\pm L}\phi\mathbf{v}\mathbf{n}d\mathbf{x} + \int_{y=\pm 1}\phi\mathbf{v}\mathbf{n}d\mathbf{x} + \sum_{i=1}^{N}\int_{\partial D_i}\phi\mathbf{v}\mathbf{n}d\mathbf{x}]\} \tag{2.9}$$

The third and the fifth integrals in (2.9) are equal to zero due to the definition the functional space W_p. Note that $\phi(\mathbf{x}) = const$ on ∂D_i.

On the horizontal boundaries $y = \pm 1$ the function ϕ takes values ± 1 respectively. We will use functions with this property hereafter. To simplify the notations we introduce the function $\phi^0(\mathbf{y}) = \pm 1$ when $y = \pm 1$. Then (2.9) takes the form

$$\hat{A} = max_{\mathbf{v}\in W_p}\{-\frac{1}{2}\int_{Q_p}\mathbf{v}^2 d\mathbf{x} + \int_{y=\pm 1}\phi^0\mathbf{v}\mathbf{n}d\mathbf{x} + min_{\phi\in V_p}[-\int_{Q_p}\phi div\mathbf{v}d\mathbf{x}]\} \tag{2.10}$$

The third term in (2.10) is linear in ϕ and it is equal to $-\infty$ if $div\mathbf{v} \neq 0$. Thus maximum in (2.10) is attained on the functions satisfying the condition $div\mathbf{v} = 0$ (see also [14]). Note that the condition $div\mathbf{v} \neq 0$ ($div\mathbf{v} = 0$) is understood in the weak sense, that is

$$\int_{Q_p}\phi div\mathbf{v}d\mathbf{x} = -\int_{Q_p}\nabla\phi\cdot\mathbf{v}d\mathbf{x}, \text{ for any } \phi \text{ with compact support.} \tag{2.11}$$

As a result we obtain

$$\hat{A} = max_{\mathbf{v}\in W_p\ ,\ div\mathbf{v}=0}\{-\frac{1}{2}\int_{Q_p}\mathbf{v}^2 d\mathbf{x} + \int_{y=\pm 1}\phi^0\mathbf{v}\mathbf{n}d\mathbf{x}\} \tag{2.12}$$

From (2.12) we get a lower bound for the effective constant

$$\hat{A} \geq J(\mathbf{v}) = \{-\frac{1}{2}\int_{Q_p}\mathbf{v}^2 d\mathbf{x} + \int_{y=\pm 1}\phi^0\mathbf{v}\mathbf{n}d\mathbf{x}\} \quad \text{for any } \mathbf{v}\in W_p \text{ such that } div\mathbf{v} = 0 \tag{2.13}$$

The solution ϕ of the problem (2.1), (2.2) satisfies(see [14]):

$$J(\mathbf{v}) = I(\phi), \tag{2.14}$$

where $\mathbf{v} = \nabla\phi$.

Equality (2.14) follows from the definition of the functionals $I(\phi)$ and $J(\mathbf{v})$ ((2.2), (2.13)) and Green's identity. Using the boundary conditions (1.4)-(1.6) this identity can be written as follows:

$$\int_{Q_p}|\nabla\phi|^2 d\mathbf{x} = \int_{y=\pm 1}\partial\phi/\partial\mathbf{n}\phi^0 d\mathbf{x} \tag{2.15}$$

2.3. Construction of the upper and lower bounds based on the solution of the discrete model from Section 1. We begin with the construction of dual bounds, which work for any distribution of the inclusion. To simplify the calculations, we consider the identical inclusions when the disks are of the same radii (the monodispersed case). All calculations can be generalized for the polydispersed case.

From (2.5) and (2.13) we have the two-side bounds for the effective constant

$$\frac{1}{2}\int_{Q_p}|\nabla\phi|^2 d\mathbf{x} \geq \hat{A} \geq -\frac{1}{2}\int_{Q_p}\mathbf{v}^2 d\mathbf{x} + \int_{y=\pm 1}\phi^0 \mathbf{v}\mathbf{n} d\mathbf{x}, \tag{2.16}$$

which hold for any test functions $\phi \in V_p$ and $\mathbf{v} \in W_p$, $div\mathbf{v} = 0$.

A successful choice of the test functions leads to the tight bounds. There is no general recipe for choosing the tight bounds since the form of of the test functions depends on the geometry, the interface conditions and the PDE. The main point of the analysis in this section is to show that *for our specific problem* we can construct the upper and the lower bounds so that they coincide to the leading order asymptotics in δ (tight bounds). The idea of constructing the tight bounds is not new and have been used by many authors but each time the main question is the actual construction of dual test functions. The latter is usually a highly nontrivial task and there is no generic approach for such a construction since it relies on specific features of the problem. For example, the test functions for the dual bounds from [9] or [24] are very different from ours (and from each other) due to different geometries.

In Section 1 we introduced the discrete network $\{x_i, g_{ij}; i, j = 1, ..., N\}$, where x_i are the sites of the network (graph) and g_{ij} are the specific fluxes (the flux from the i-th to the j-th disk given by formula (1.19)). Our goal is to obtain asymptotic formulas for the functionals in the two-side bounds (2.16) such that the leading terms are expressed in terms of the network problem parameters: the specific fluxes g_{ij} and the potentials t_i on the sites x_i. We shall next formulate the conditions under which the leading terms are the same and therefore the bounds provide the leading term in the asymptotic expansion for the effective coefficient $\hat{A}$ (compare with the Squeeze Theorem).

The test functions are constructed in some neighborhoods of the disks and for a pair of neighboring disks. In order to define the notion of a neighboring disk we shall employ Voronoi construction. This construction will also allow us to introduce the interparticle distance parameter, which will be used in the justification of the asymptotic formula. To this end we first recall the notion of the two-dimensional Voronoi tessellation. It is illustrated by Fig. 2.1, where the boundaries of the polygons are formed from the points which are equidistant from the given set of sites x_i. Thus the Voronoi polygon (more precisely its interior) of the site x_i is the set of all points which are closer to the site x_i than to any other site x_j, $j \neq i$. This definition works for the set of points (sites) of an infinite plain.

It also can be adopted for a set of points (sites) inside our rectangular domain Π. It could be done in a number of ways, for example, by the symmetric reflecting of the domain Π and set of sites x_i about each edge of Π followed by restriction of the Voronoi cells in the broader domain ("4Π") to the original domain Π.

2.4. The lower bound. Due to (2.16) the effective coefficient can be bounded from below by

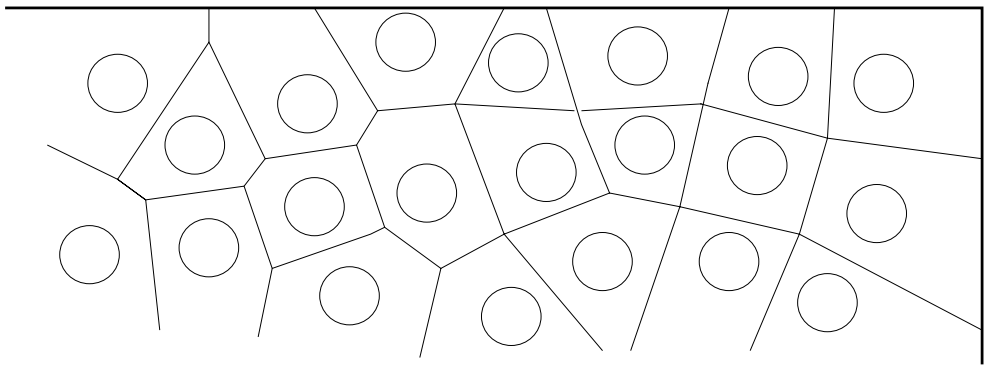

FIG. 2.1. *Voronoi tessellation*

$$\hat{A} \geq J(\mathbf{x}) = -\frac{1}{2}\int_{Q_p} \mathbf{v}^2 d\mathbf{x} + \int_{y=\pm 1} \phi^0 \mathbf{v}\mathbf{n} d\mathbf{x}, \tag{2.17}$$

where the test function $\mathbf{v}$ satisfies the following conditions

$$div\mathbf{v} = 0 \text{ in } Q_p \tag{2.18}$$

$$\int_{\partial D_i} \mathbf{v}\mathbf{n} d\mathbf{x} = 0,\ i = 1, ..., N \tag{2.19}$$

From the physical point of view both conditions mean that there are no sources and sinks. Condition (2.18) holds for the matrix (perforated domain) Q_p and it is a local (differential) condition. The integral condition (2.19) holds for each inclusion D_i and for $\mathbf{v} \in L_2$ it can be understood in the distributional sense (e.g. for $\mathbf{v} \in L^2(D)$ and divergence free, one defines $\mathbf{v} \cdot \mathbf{n}$ as a distribution on the boundary of D by $\int_{\partial D} \mathbf{v}\mathbf{n}\phi = \int_D \mathbf{v} \operatorname{grad} \phi$). Also

$$\mathbf{v}\mathbf{n} = 0 \text{ on the surface } x = \mp L \tag{2.20}$$

since there is no flux through the vertical boundaries $y = \mp 1$ (insulating conditions, see (2.6)).

Construction of the test function for the dual problem

We now construct the test function for the functional (2.17). It is based on some properties of the solution of the network problem which were presented in Section 1. Consider two disks (i-th and j-th) as shown in Fig. 2.2. The choice of the coordinate system as shown in Fig.2.2 does not lead to a loss of generality because all quantities in the formulas (2.17)-(2.20) are invariant with respect the rotation of the coordinate system. We will construct the test function in the neck Π_{ij}. The neck is chosen so that it does not overlap with any other neck attached to the same inclusion (if any other neck exists) and does not intersect any other disk. More specific conditions on the will be presented below.

We choose the test function in the form

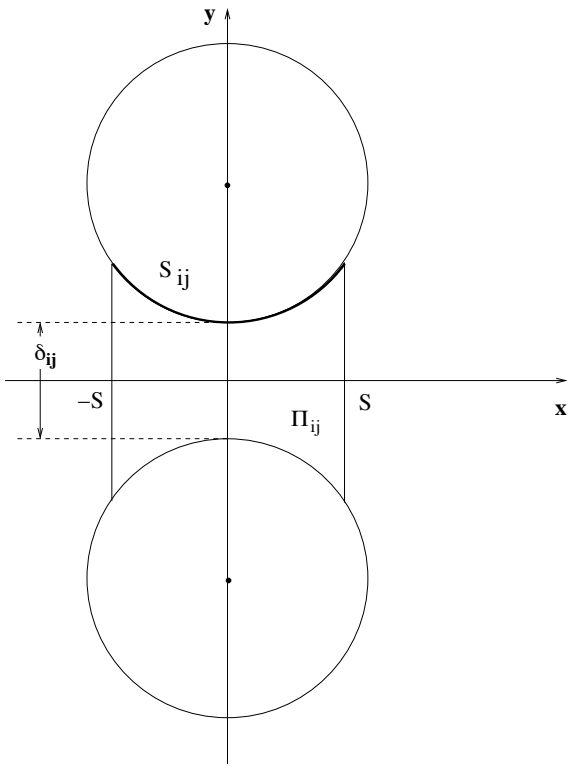

FIG. 2.2. *The "neck" between two disks*

$$\mathbf{v} = \begin{cases} (0, \zeta(x)) & \text{in the neck } \Pi_{ij}, \\ (0,0) & \text{otherwise} \end{cases} \tag{2.21}$$

Here $\zeta(x)$ is a smooth function of a single variable x. We need to make sure that it is in the class of admissible functions. To this end we note that it satisfies (2.18) since

$$div\mathbf{v} = 0 + \partial\zeta/\partial y = 0 \tag{2.22}$$

Note that $\mathbf{v}$ is only piecewise smooth but the div operator does not lead to δ-functions because $v_1 \equiv 0$ and we differentiate $v_2(x)$ in y.

Substitute (2.21) into the integral (2.19). For this function we integrate only over the arc $S_{ij} \in D_i$. Then the flux of the vector $\mathbf{v}$ through the curve $S_{ij} \in \partial D_i$ is equal to

$$\int_{S_{ij}} \mathbf{v}\mathbf{n} d\mathbf{x} = \int_{-S}^{S} \mathbf{v}\mathbf{n} dx = \int_{-S}^{S} \zeta dx \tag{2.23}$$

The first equality in (2.23) follows from the divergence theorem, equality (2.22) and the fact that $\mathbf{v}\mathbf{n} = 0$ on the lateral sides of the neck for functions of the form (2.21).

We have discussed here the case of two disks (i-th and j-th). In general the i-th disk has several neighbors and due to (2.19)

$$\int_{\partial D_i} \mathbf{v}\mathbf{n}d\mathbf{x} = \sum_j \int_{S_{ij}} \mathbf{v}\mathbf{n}d\mathbf{x} \tag{2.24}$$

since the test function is of the form (2.21).

Thus equations (2.19)-(2.24) are some sort of balance equations (the sum of all integral fluxes into the given disk from all neighbors is equal to zero). The test function (2.21) is constructed so that all fluxes can flow through the necks (channels) only. The flux through each neck is given by (2.23) and we need to consider all necks between neighbors. So we need to choose our test function so that for each inclusion the balance equation (2.19) holds. In other words we need a set of numbers which can be chosen as corresponding integral fluxes. Where do we get such set of numbers? In short, the answer is in the discrete problem, where such set of numbers have been constructed.

Indeed, let us revisit the network problem (Section 1, (1.25)). Consider the set of numbers (the current flux)

$$p_{ij} = g_{ij}(t_i - t_j), \tag{2.25}$$

where $\{t_i\}$ are the solutions of the algebraic system (1.25), the numbers $\{g_{ij}\}$ (integral values of the specific fluxes between neighbors) are defined in Section 1 (see (1.19)). Then the equation (1.25) has the form of the Kirchhoff's current law

$$\sum_{j=1}^{N} p_{ij} = 0 \ , \ i \in I. \tag{2.26}$$

In order to satisfy the balance equation (2.19) on ∂D_i and condition (2.20) it is sufficient to impose the following condition the test function $\mathbf{v}$ $(\zeta(x))$:

$$\int_{-S}^{S} \zeta_{ij}(x)dx = p_{ij}, \tag{2.27}$$

Note that (2.27) holds for the $ij-th$ neck and to simplify notations we shall skip the subscripts ij when construct $\zeta(x)$.

Construction of the function function $\zeta(x)$, which determines the test function.

Recall that we are analyzing the lower bound (2.17) and our goal is to make it as tight as possible, which means that we wish to increase the right-hand side of (2.17). The latter can be achieved by decreasing the value of the integral $\int_{\Pi_{ij}} \mathbf{v}^2 d\mathbf{x}$, which for the test function (2.21) writes as follows

$$\int_{-S}^{S} \zeta^2(x)H(x)dx, \tag{2.28}$$

where $H(x)$ is the distance between the disks (see Fig.4.1).

Minimization of the integral (2.28) is to be carried out under the constraints (2.27). Therefore we need to use the Lagrange multiplier λ in the corresponding Euler-Lagrange equation:

$$2\zeta(x)H(x) - \lambda = 0. \tag{2.29}$$

From (2.29) we obtain

$$\zeta(x) = \frac{\lambda}{H(x)} \tag{2.30}$$

where λ is an unknown multiplier to be determined (clearly factor 2 in (2.29) can be dropped).

The equality (2.30) implies that the desired test function (which determines the local flux) is inversely proportional to the distance between the disks. The latter agrees with the physical assumptions about the flux between two closely spaced disks formulated in [20] and the asymptotic solution of Laplace equation in [27].

Substituting (2.30) into (2.27) we obtain

$$\int_{-S}^{S} \lambda \frac{dx}{H(x)} = p_{ij} = g_{ij}(t_i - t_j), \tag{2.31}$$

where the numbers p_{ij} have been defined in (2.25).

Introduce the following quantities

$$g^s_{ij} = \int_{-S}^{S} \frac{dx}{H(x)}. \tag{2.32}$$

From (2.31) we obtain

$$\lambda g^s_{ij} = p_{ij}$$

or

$$\lambda = \frac{p_{ij}}{g^s_{ij}} = \frac{g_{ij}(t_i - t_j)}{g^s_{ij}} \tag{2.33}$$

If we choose λ according to (2.33), then the test function $\mathbf{v}$ defined by (2.21),(2.30) satisfies all conditions (2.18)-(2.20).

Substitute (2.30), (2.33) into the integral

$$\int_{\Pi_{ij}} -\frac{1}{2}\mathbf{v}^2 d\mathbf{x}$$

over the neck Π_{ij}. Since the integrand does not depend on the variable y, we evaluate the latter integral as follows:

$$\begin{aligned} \int_{-S}^{S} \zeta^2(x)H(x)dx &= \int_{-S}^{S} (\frac{\lambda}{H(x)})^2 H(x)dx \\ &= \lambda^2 \int_{-S}^{S} \frac{dx}{H(x)} = \lambda^2 g^s_{ij} = \frac{g^2_{ij}(t_i - t_j)^2}{g^s_{ij}} \end{aligned} \tag{2.34}$$

This calculation is for a pair of disks. Consider now all the disks in the composite. Recall that this set also includes the quasidisks, therefore the set of all the disks D_i can be decomposed into two disjoint sets: the set of internal disks denoted by I and the set of the boundary disks, which is the union of all disks which intersect the boundaries $y = \pm 1$ and the "quasidisks"(those two sets are denoted by S^+ and S^- respectively). The "quasidisks" incorporate information about the interaction between the boundary of the domain Π and the internal disks and they can be treated as disks of radius $R = \infty$ (see Fig. 4.2). Thus all calculations for the disks and the "quasidisks" have been carried out using the same formulas and from the mathematical point of view there are no reasons to make differences between the disks and the "quasidisks". But it is important to take into account difference in enumeration of the disks and the "quasidisks". In particular, the "quasidisks" belong to the sets $S^{\pm}$ (horizontal boundaries) only. We also remark that the disks which intersect boundary are treated as regular disks with the potential ± 1.

By previous remarks equation (2.22) should be understood in the weak sense; however for the chosen test functions one can check directly that the divergence-free condition as well as the boundary conditions in the classical sense yield the same result. Indeed, our test function (v_1, v_2) is vectorial and moreover $v_1 = 0$ everywhere, and v_2 is discontinuous. However,v_2 depends on x only which is why the differentiation in y ($\partial v_2/\partial y = 0$) does not lead to the δ-function, which agrees with the physical picture.

We now evaluate the functional (2.17). It consists of the double and the boundary integrals.

Calculation of the double integral in (2.17).

The integral

$$\int_{\Pi_{ij}} -\frac{1}{2}\mathbf{v}^2 d\mathbf{x}$$

over one neck Π_{ij} have been evaluated above. Since in our construction different necks do not overlap, this evaluation amounts to the summation of the integrals over all necks Π_{ij} (for both the disks and the "quasidisks"). Furthermore, the integral over one neck is given by (2.34) and therefore we get

$$\int_{Q_p} -\frac{1}{2}\mathbf{v}^2 d\mathbf{x} = -\frac{1}{2}\sum_{\Pi_{ij}} \frac{g_{ij}^2 (t_i - t_j)^2}{g_{ij}^s} \tag{2.35}$$

Index Π_{ij} in the sum means that we sum up over the necks. When change to the summation over the indices $i, j = 1, ..., N$ (N is the number of disks) we will count each neck Π_{ij} twice. Therefore a factor $\frac{1}{4}$ appears in the sum over i, j instead of $\frac{1}{2}$ in (2.35). Then we write (2.35) in the form

$$\int_{Q_p} -\frac{1}{2}\mathbf{v}^2 d\mathbf{x} = -\frac{1}{4}\sum_{i,j=1}^{N} \frac{g_{ij}^2 (t_i - t_j)^2}{g_{ij}^s} \tag{2.36}$$

Alternatively one can sum up over $i \leq j$=$1, ..., N$, then the factor $\frac{1}{2}$ still will be in place. We pay attention to these technical issues because our goal is to make sure that the leading terms of the direct and dual functionals are actually the same.

Calculation of the boundary integral in (2.17).

The flux **vn** through the boundary $y = \pm 1$, where the test function defined by (2.21), (2.30), is given by

$$\mathbf{vn} = \frac{\lambda}{H(x)} \tag{2.37}$$

Here we have used the function $\phi^0(y) = \pm 1$ when $y = \pm 1$, which have been introduced earlier.

Using (2.37), (2.33) and the definition of $\phi^0(y)$, we compute the integral $\int_{y=\pm 1} \phi^0 \mathbf{vn} d\mathbf{x}$:

$$\sum_{\Pi_{ij}} \int_{-S}^{S} \frac{\lambda dx}{H(x)} = \sum_{\Pi_{ij}} \lambda \int_{-S}^{S} \frac{dx}{H(x)} = \sum_{\Pi_{ij}} \frac{g_{ij}(t_i - t_j) g_{ij}^s}{g_{ij}^s} = \sum_{\Pi_{ij}} g_{ij}(t_i - t_j)$$

Here we sum only over the necks Π_{ij} adjacent to the boundary y=+1. If $i \in S^+$ (S^+ is the set of the disks and "quasidisks" adjacent to the boundary $y = +1$) then we do not count any neck twice as it was the case in the double integral.

Then the integral over the boundary $y = +1$ in (2.17) is given by

$$P^+ \equiv \sum_{i \in S^+ j=1,\ldots,n} g_{ij}(t_i - t_j) \tag{2.38}$$

Integral over the boundary $y = -1$ in (2.17) can be evaluated similarly ($\phi^0(y) = -1$ when $y = -1$) and it is given by

$$P^- \equiv \sum_{i \in S^- j=1,\ldots,n} g_{ij}(t_i - t_j) \tag{2.39}$$

The sums (2.38) and (2.39) represent fluxes through the boundaries S^+ and S^- respectively (S^+ and S^- correspond to $y = \pm 1$ in the continuum model) in the discrete network model, which have been introduced in Section 1. Note that due to the conservation of flux they are equal.

We introduce notations P^+ and P^- for the fluxes (2.38) and (2.39) by P^+ and P^- respectively.

So, we have evaluated both integrals in (2.17) for the test function (2.21) and we arrived at the following

PROPOSITION 2.1.

$$\hat{A} \geq J(\boldsymbol{v}) = -\frac{1}{4} \sum_{i,j=1}^{N} \frac{g_{ij}^2 (t_i - t_j)^2}{g_{ij}^s} + (P^+ - P^-) \tag{2.40}$$

where g_{ij}^s and g_{ij} are defined in (2.32) and in (1.19) respectively; P^+ and P^- are given by (2.38) and (2.39) respectively.

To understand the "-" sign in the RHS of (2.40) one should look at (2.15) and the definition of the function ϕ^0.

2.5. The upper bound. Our goal is to construct a **test function**, which mimics the behavior of the exact solution and substitute it into the following inequality (see (2.16))

$$\hat{A} \le J(\mathbf{v}) = \frac{1}{2}\int_{Q_p} |\nabla\phi|^2 d\mathbf{x}, \tag{2.41}$$

where $\phi \in V_p$. We shall use the knowledge gained in the developing of the network model in Section 2. Roughly speaking the test function behaves according to the Keller's approximation in a narrow neck between each two closely spaced disks and outside these neck we make a prolongation. Then the integral in the RHS of (2.41) will be decomposed into two parts: first part is due to the contribution from the necks, and the second part is the contribution from the prolongation. It will be shown that the first part is precisely the network approximation and the second part is much smaller than the first part, when the disks are closely packed. We will use the notion of the Voronoi tessellation to formulate the close-packing condition (CPC)

Any test function should be piecewise-differentiable and satisfy the other conditions in the definition of the space V_p (2.1). In particular, it means that the test function takes constant values on the disks D_i and is equal to ± 1 on the boundaries $S^{\pm}$. Let us consider two disks (i-th and j-th, see Fig.2.3). The choice of the coordinate system in the Fig.2.2 is not important because the integral in (2.41) is invariant under any rotation of the coordinate system.

We first describe a sketch of the construction of the test function. We need to ensure that the test function takes values t_i and t_j on the disks D_i and D_j. In fact, it is sufficient for the function to take these values on the boundaries ∂D_i and ∂D_j and to be smooth (H^1) outside the disks. Again consider the neck Π_{ij} (connecting the i-th and the j-th disks). In this neck the test function changes linearly from t_i to t_j when moving from the disk D_i to the disk D_j (Keller's approximation for two closely spaced disks). Next we extend the test function into VORONOI CELL. Next we describe the construction of the test function in each subdomain of Fig. 2.4

Construction in the neck Π_{ij}

From the physical point of view the flux (the field) in the narrow channel (the neck Π_{ij}) must be linear in y, see [20]. This motivates us to take the test function ϕ linear in y in the neck Π_{ij} with the values t_i and t_j on the disks ∂D_i and ∂D_j (or, which is the same, for $y = -H(x)/2$ and $y = H(x)/2$) respectively. These conditions uniquely determine the function ϕ of the form

$$\phi(x,y) = t_i + \frac{(t_j - t_i)(y + H(x)/2)}{H(x)} = t_i + (t_j - t_i)(\frac{y}{H(x)} + \frac{1}{2}),\ y \in [-H(x)/2, H(x)/2] \tag{2.42}$$

The partial derivatives of the function (2.42) are given by

$$\partial\phi/\partial x = -(t_j - t_i)\frac{yH'(x)}{H^2(x)} \tag{2.43}$$

$$\partial\phi/\partial y = \frac{t_j - t_i}{H(x)} \tag{2.44}$$

where $'=d/dx$.

We need to evaluate $\int_{Q_p} |\nabla\phi|^2 d\mathbf{x}$. For ϕ given by the equation (2.44) we have

$$\int_{\Pi_{ij}} (\partial\phi/\partial y)^2 dxdy = \int_{-S}^{S} \frac{(t_j - t_i)^2}{H^2(x)} H(x)dx = (t_j - t_i)^2 g_{ij}^s \tag{2.45}$$

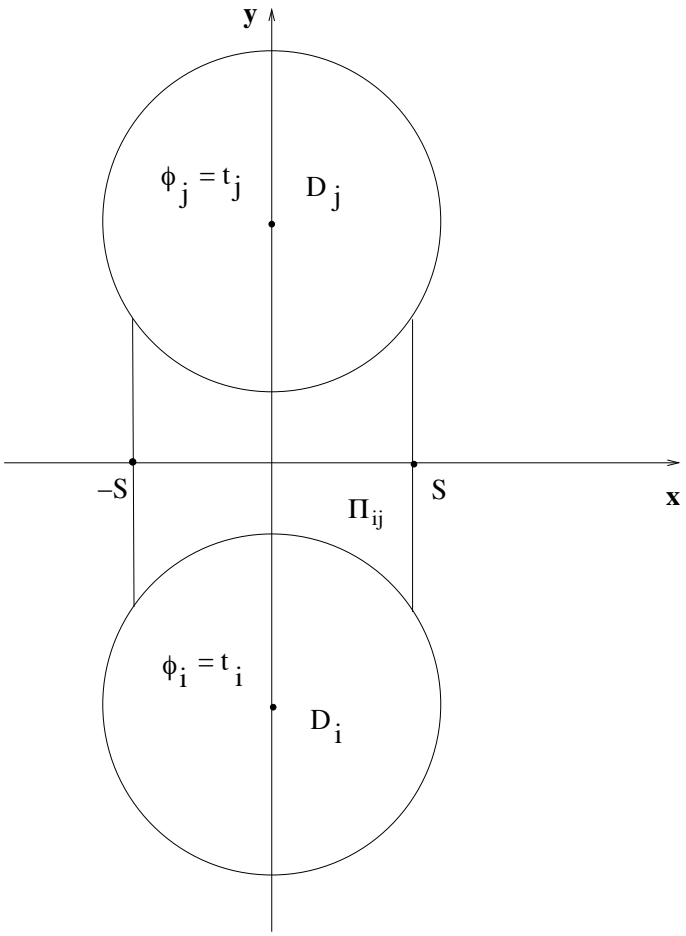

FIG. 2.3.

In (2.45) we switch from the double integral to the iterated integral. Since $\partial\phi\,/\partial y$ (2.44) does not depend on y, we arrive to the integral in the variable x where the integrand is multiplied by $H(x)$. Recall that

$$\Pi_{ij} = \{(x,y) : x \in (-S,S),\ -H(x)/2 \le y \le H(x)/2\} \tag{2.46}$$

For (2.43) we have

$$\int_{\Pi_{ij}} (\partial\phi/\partial x)^2 dxdy = \int_{\Pi_{ij}} (t_j - t_i)^2 (\frac{yH'(x)}{H^2(x)})^2 dxdy$$

Since $|y/H(x)| \le 1/2$ (see, (2.46)), the last integral is bounded by the following quantity

$$(t_j - t_i)^2 \int_{\Pi_{ij}} (\frac{y}{H(x)})^2 \frac{H'^2(x)}{H^2(x)} dxdy \le \frac{(t_j - t_i)^2}{4} \int_{\Pi_{ij}} \frac{H'^2(x)}{H^2(x)} dxdy = \frac{(t_j - t_i)^2}{4} \int_{-S}^{S} \frac{H'^2(x)}{H(x)} dx \tag{2.47}$$

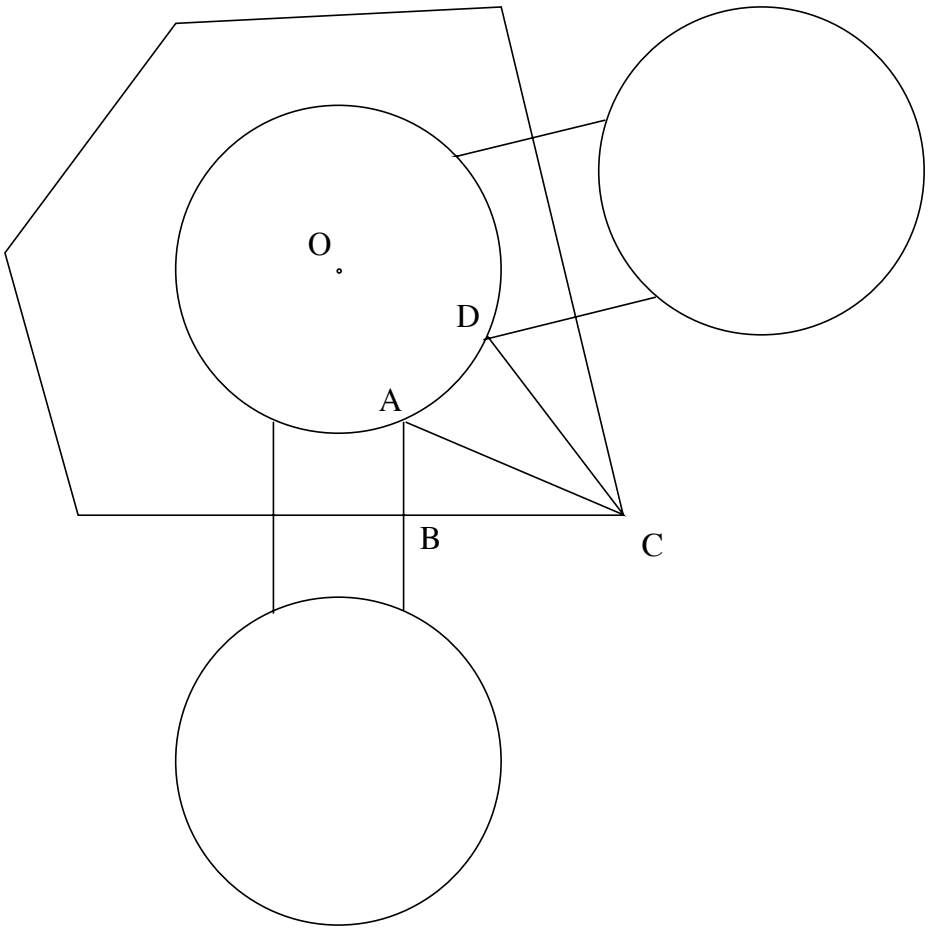

FIG. 2.4. *Decomposition of Voronoi cell*

In the last equality in (2.47) we again reduce the double integral to the integral in x, using the fact that the integrand in the second integral in (2.47) does not depend on the variable y, which leads to the multiplication of the integrand by $H(x)$. Since $H(x) = \delta + 2R - 2\sqrt{R^2 - x^2}$, the integrand in (2.47) is given by

$$\frac{H'^2(x)}{H(x)} = \frac{4x^2}{R^2 - x^2} \frac{1}{\delta + 2R - 2\sqrt{R^2 - x^2}} \leq \tag{2.48}$$

$$\frac{2}{R^2 - x^2} \frac{x^2}{R - \sqrt{R^2 - x^2}} = \frac{2}{R^2 - x^2}(R + \sqrt{R^2 - x^2}) = \frac{2R}{R^2 - x^2} + \frac{2}{\sqrt{R^2 - x^2}}$$

If we restrict the thickness of neck with the natural condition

$$S \leq R/2, \tag{2.49}$$

then the last expression in (2.48) is bounded .

The maximum of the last expression in the RHS of (2.48) in the interval (2.49) is denoted by C. Then the constant C does not depend on δ and the integral (2.47) is bounded by the quantity

$$E_A = \frac{(t_i - t_j)^2}{4} C \cdot 2S, \tag{2.50}$$

which does not depend on δ. Here we have used the discrete maximum principle (Lemma 1.3), which implies that $t_i,\ t_j$ are uniformly bounded independent on δ.

B. Construction in the triangle ABC

In the triangle ABC (see Fig.2.4) we construct a linear function ϕ which takes the following values: t_i in the point A, $(t_i + t_j)/2$ at the point B and 0 at the point C.

In the coordinate system $0XY$ oriented so that OX and OY are parallel to the legs BC and AB respectively centered at the point B we have

$$\phi = \alpha x + \beta y + \gamma$$

It is clear that $\gamma = (t_i + t_j)/2$ and we satisfy the condition at the point B.

Then the above conditions at A and C imply

$$\alpha |BC| + \gamma = 0,\ \beta |AB| + \gamma = t_i,$$

Solving this system, we obtain

$$\alpha = -\frac{\gamma}{|BC|}, \beta = -\frac{\gamma}{|AB|} + \frac{t_i}{|AB|}$$

Then

$$\phi = \frac{t_i + t_j}{2}(-\frac{x}{|BC|} + 1) - \frac{t_i - t_j}{2}\frac{y}{|AB|} \tag{2.51}$$

For the function (2.51) we have

$$\nabla\phi = (-\frac{t_i + t_j}{2}\frac{1}{|BC|}, -\frac{t_i - t_j}{2}\frac{1}{|AB|})$$

and the integral

$$\int_{ABC} \frac{1}{2}|\nabla\phi|^2 d\mathbf{x} = (\frac{(t_i + t_j)^2}{8}\frac{1}{|BC|^2} + \frac{(t_i - t_j)^2}{8}\frac{1}{|AB|^2})|ABC|, \tag{2.52}$$

where $|ABC|$ stands for the area of the triangle ABC. Simple geometrical considerations provide independent of δ lower bounds for $|AB$ and $|BC|$. These bounds are presented in the Appendix 1.

Then $BC \geq const$, where $const > 0$ does not depend on δ and the quantities in the RHS of (2.52) do not depend on δ as $\delta \to 0$. The quantities t_i also do not depend δ (see Lemma 1.3.

Then from (2.52) we have

$$\int_{ABC} \frac{1}{2}|\nabla\phi|^2 d\mathbf{x} \le C_1|ABC| \tag{2.53}$$

where C_1 does not depend δ .

C. Constructing the test function in the triangle ACD.

The function ϕ is linear on the sides AC and DC. Moreover it takes the value t_i at A and D (and along the whole arc AD) and the value 0 at C. we extend this function into the curvilinear triangle ADC by taking ϕ of the form

$$\phi = \alpha\rho + \delta \tag{2.54}$$

and the following conditions hold

$$\alpha R + \delta = t_i, \alpha|OC| + \delta = 0,$$

where O is the center of the disk under consideration, R is the radius of the disk and ρ is the polar coordinate (polar radius), which corresponds to the center O.

Solving this system, we have

$$\alpha = -\frac{t_i}{(1 - R/|OC|)|OC|}, \delta = \frac{t_i}{1 - R/|OC|} \tag{2.55}$$

For the function (2.54),(2.55) we have

$$\int_{ADC} \frac{1}{2}|\nabla\phi|^2 d\mathbf{x} = \int_{adc} \frac{1}{2}[(\partial\phi/\partial\rho)^2 + \frac{1}{\rho}(\partial\phi/\partial\Theta)^2]\rho d\rho d\Theta = \int_{adc} \frac{1}{2}\alpha^2 \rho d\rho d\Theta = \frac{1}{2}\alpha^2|ADC| \tag{2.56}$$

where ρ, Θ are the polar coordinates and the domain abc corresponds to the triangle ABC in the polar coordinate system.

The quantity $|OC| \ge L$, where L is the length of the leg of the right triangle which encircles the disk. Then $R/|OC| \le R/L < 1$ and R/L does not depend on δ.

Due to (2.55),(2.57) and Lemma 1.3 we have

$$\int_{ABC} \frac{1}{2}|\nabla\phi|^2 d\mathbf{x} \le C_2|ABC| \tag{2.57}$$

where C_2 does not depend δ .

D. The boundary disks. After we have introduced Voronoi tessellation, we can define the quasidisks as the segments obtained by partitioning the boundary $y = \pm 1$ by Voronoi cells. Then the quasidisks again can be considered as disks with an infinite radius for the purpose of calculating the flux according to the Keller's formula ((1.19)). The length of the quasidisk is not essential and therefore this definition is equivalent to the definition of a quasidisk introduced in Section 1.

For a boundary disk (or equivalently for a pair disk-quasidisk) the boundary of the domain Π is also the boundary of the Voronoi cell. Therefore we can not require

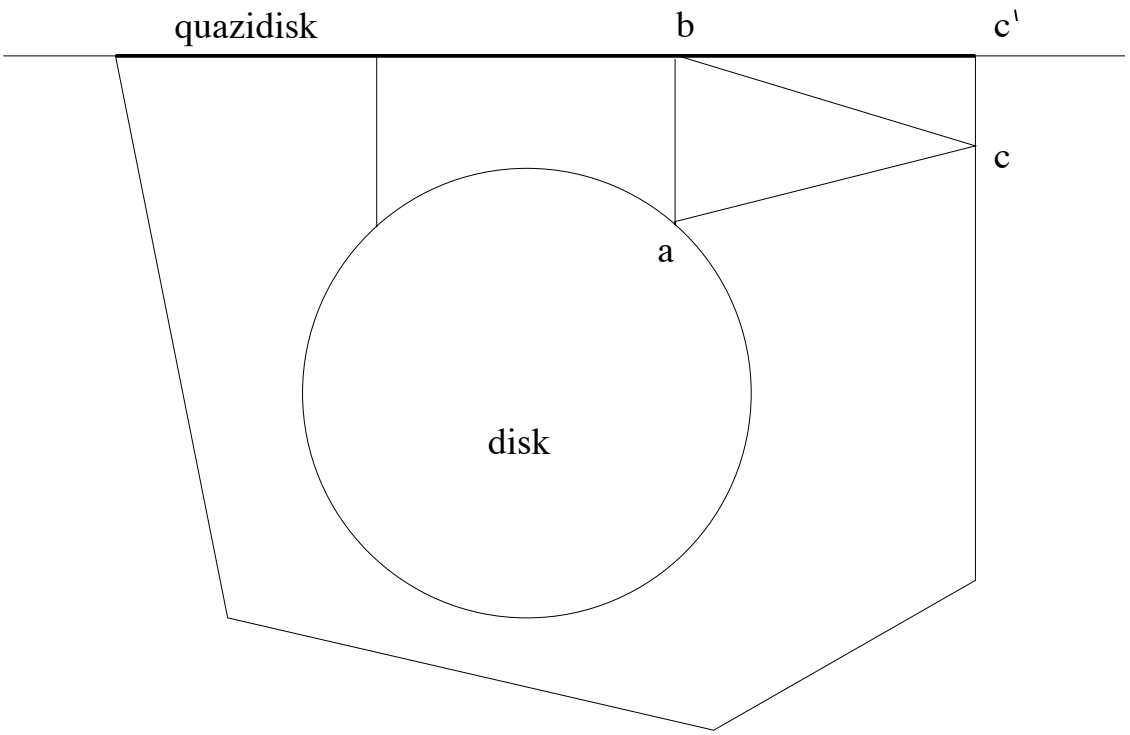

FIG. 2.5. *Boundary disk*

$\phi = 0$ at c' (see Fig.2.5). However, the above construction works if we introduce a site (node) c at the distance $\sqrt{R^2 - S^2}/2$ from the boundary (see Fig.2.5) and require $\phi = 0$ at c. Then in the triangle $bc'c$ we construct a liner function with values 1 on bc' and 0 at c. It is given by

$$\phi = 1 - \frac{y}{|cc'|}$$

For this function we have

$$\int_{bc'c} \frac{1}{2}|\nabla\phi|^2 d\mathbf{x} = \int_{bc'c} \frac{1}{2|cc'|^2} = \frac{1}{R^2 - S^2}|bc'c|$$

The quantity $S > 0$ does not depend δ and therefore we have

$$\int_{bc'c} \frac{1}{2}|\nabla\phi|^2 d\mathbf{x} \leq C_3|bc'c| \tag{2.58}$$

where C_3 does not depend δ .

E. Evaluation of the Dirichlet integral outside the necks.

The domain outside the disks can be decomposed into the set of necks and the set of triangles (see Fig.2.4), which have been considered in the steps $A - D$. We denote by U the domain outside the disks and necks.

From (2.53), (2.57) and (2.58) we have

$$\int_U \frac{1}{2}|\nabla\phi|^2 d\mathbf{x} \le max(C_1, C_2, C_3)|U| \tag{2.59}$$

where $|U|$ stands for the area of the domain U . It is clear that $|U|$ is less than the area of the domain Q_p

Using (2.59), we can write

$$\int_U \frac{1}{2}|\nabla\phi|^2 d\mathbf{x} \le C|\Pi| \tag{2.60}$$

where the constant C does not depend on δ, $|\Pi|$ is the area of the domain Π.

Summing up over all necks and triangles, we obtain

$$\int_{Q_p} \frac{1}{2}|\nabla\phi|^2 d\mathbf{x} = \frac{1}{4}\sum_{i,j=1}^{N} g_{ij}^s (t_i - t_j)^2 + \sum_{\Pi_{ij}} \int_{\Pi_{ij}} \frac{1}{2}|\partial\phi/\partial x|^2 d\mathbf{x} + \int_U \frac{1}{2}|\nabla\phi|^2 d\mathbf{x} \tag{2.61}$$

The factor $\frac{1}{4}$ in (2.61) appears by the same reason as in (2.36): it is the double counting of the necks when summing up in $i, j = 1, ..., N$. In order to keep the usual factor $\frac{1}{2}$ in (2.61) one can sum up over $i < j$. As a result from (2.60) and (2.61) we obtain

Proposition 2.2.

$$\hat{A} \le \frac{1}{4}\sum_{i,j=1}^{N} g_{ij}^s (t_i - t_j)^2 + M \tag{2.62}$$

where g_{ij}^s are defined in (2.32), and the constant $M = max(C_1, C_2, C_3)|U| + NE_A$ is uniformly bounded in δ. Here N is the number of disks, and E_A is defined in (2.50)

2.6. Justification of the approximation of the continuum model by the discrete network for closely packed disks. In this subsection we prove that when the relative interparticle distance δ/R goes to 0, the upper and the lower bounds obtained above coincide to the leading order. Thus we obtain an asymptotic formula for the effective constant $\hat{A}$ in terms of the characteristics of the discrete network, which were introduced in Section 1 based on physical considerations.

We now introduce the interparticle distance parameter, which will be used in the justification of the asymptotic formula. It is based on the notion of Voronoi tessellation, which was presented above (see also Fig. 2.1).

In the context of our problem we shall do the following. Given a set of randomly distributed disks in the domain Π, we take the centers x_i as the sites of the Voronoi tessellation of Π. Then the neighboring Voronoi polygons (cells) determine the neighboring disks (neighboring cells share a common edge). We connect the neighborings sites x_i and x_j by segments $x_i\, x_j$. We then connect the sites near the boundary of Π (centers of the disks which lie near the boundary) with the boundary by perpendiculars from this centers to the corresponding (nearest) edges of Π. Here we have treated

pieces of the boundaries as quasidisks Thus we have constructed a graph, denote it by $G(\Pi)$. Note that this graph is connected.

We next denote by δ_{ij} the length of the piece of the segment $x_i\ x_j$, which is located outside the neighboring disks D_i and D_j (Fig.) and introduce the maximal packing distance $\delta = max\ \delta_{ij}$, where the maximum is taken over all neighbors (including the quasidisks). Consider a sequence of graphs $G_n(\Pi)$ and the corresponding sequence of the maximal packing distances δ_n.

DEFINITION 2.3. *We say that the sequence of graphs $G_n(\Pi)$ satisfies the* δ **close packing condition** *if $\delta_n \to 0$ as $n \to \infty$.*

We shall use this definition in the main theorem of this Section.

Note that this definition does not cover all possible closely packed configurations and it could be generalized by considering more complicated tessellation. In particular, this definition works well when the vertices of the Voronoi polygons are triple junctions as in the hexagonal tessellation. Since the hexagonal tessellation is the densest on the plane, it is of particular importance from the practical point of view. Also in the case when the δ-CPC condition in actual composite with closely packed particles does not apply to the entire composite, it can be used for large pieces of the composites (clusters in the percolation theory terminology). Then the homogenization based on the network approximation should be done for each densely packed piece (cluster).

We now show that if the close packing condition holds, then the upper and lower bounds coincide to the leading term as $\delta \to 0$.

From the bounds (2.40) and (2.62) we get

$$\hat{A} \geq -\frac{1}{4}\sum_{i,j=1}^{N} \frac{g_{ij}^2 (t_i - t_j)^2}{g_{ij}^s} + (P^+ - P^-) \tag{2.63}$$

$$\hat{A} \leq \frac{1}{4}\sum_{i,j=1}^{N} g_{ij}^s (t_i - t_j)^2 + M \tag{2.64}$$

where M is uniformly bounded in δ,

$$g_{ij}^s = \int_{-S}^{S} \frac{dx}{H(x)},$$

and $H(x)$ is the (local) distance between the neighboring disks as a function of x (see Fig. 1.2 with $R_i = R_j = R$)

$$H(x) = \delta_{ij} + 2R - R\sqrt{R^2 - x^2}$$

(for the i-th and the j-th disks)

$$g_{ij} = \pi\sqrt{\frac{R}{\delta_{ij}}}' \tag{2.65}$$

δ_{ij} is the minimal distance between the i-th and the j-th disks, see Fig.2.3, S is the half-width of the necks Π_{ij}.

So far we have not defined the width S of the necks uniquely . In order to do this we first summarize all restrictions on S which were introduced above:

- $S > 0$ and does not depend on δ;
- 2) $S < R/2$, see (2.49) and the necks, which corresponds to different neighbors do not overlap

Thus one can say that S is a positive number, which does not depend on δ , chosen in such a way that the necks do not overlap at least for sufficiently small δ/R. We next specify what "at least for sufficiently small δ/R" means. We choose $\delta \leq R$. This choice is not unique and is motivated by the fact that the width of the neck grows when the disks become closer. Consider two disks for which $\delta = R$, Fig. 2.6. Choose the thickness S as shown on Fig. 2.6. The choice of the tangential rays on this figure is due to the fact that the third disk can not squeeze into the wedge between the two tangential rays, in other words there is no way for a third disk to overlap with the neck on Fig. 2.6.

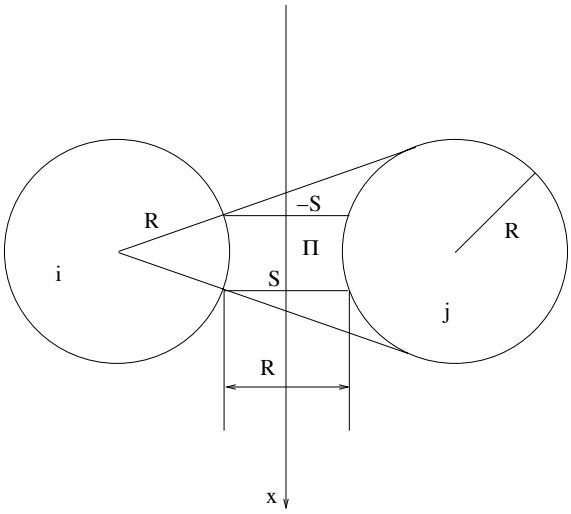

FIG. 2.6. *The width S of a neck*

Then for any smaller value of δ (the disks are coming together) the quantity S satisfies all the above conditions. So we can choose S according Fig. 2.6 that is $S = R\ arctg(1/3) \approx 0.3R$ (see also Appendix 1).

We shall need several auxiliary facts. First we establish a relation between the quantities g^s_{ij} (2.64) and g_{ij} (2.65). The first quantities came from the rigorous bounds for $\hat{A}$, the others appeared when we constructed the network in Section 1.

LEMMA 2.4. *Let δ_{ij}/R be the relative interparticle distance between the i-th and the j-th disks. Then as $\delta_{ij} \to 0$*

$$g^s_{ij} = g_{ij} + O(1) + \sqrt{\frac{R}{\delta_{ij}}} O(\delta_{ij}/R), \tag{2.66}$$

where $g_{ij} = \pi\sqrt{\frac{R}{\delta_{ij}}} \to \infty$ as $\delta_{ij} \to 0$.

Proof. For the circular disks (i-th and j-th) of radius R we have $H(x) = \delta_{ij} + 2R - \sqrt{R^2 - x^2}$. Then

$$g^s_{ij} = \int_{-S}^{S} \frac{dx}{\delta_{ij} + 2R - \sqrt{R^2 - x^2}} = \int_{-S^*}^{S^*} \frac{Rcos\alpha d\alpha}{\delta_{ij} + 2R - Rcos\alpha},$$

where we make the change of variables $x = Rcos\alpha, S^* = arcsin(S/R) > 0$. Note that S^* does not depend on δ_{ij} The last integral is equal to [Gradstein and Rizik, Integarl Tables,2.554.1, 2.555.3]

$$-\frac{1}{2} + \frac{2(\delta_{ij}+2R)}{\sqrt{(\delta_{ij}+2R)^2-4R^2}}\ arctg(\frac{\sqrt{(\delta_{ij}+2R)^2-4R^2}\ tg\alpha}{\delta_{ij}})|_{-S^*}^{S^*}$$

Consider this integral for small δ_{ij}. Keep the terms of order δ_{ij} and neglect δ_{ij}/R, we obtain

$$-\frac{1}{2} + \sqrt{\frac{R}{\delta_{ij}}}arctg(\sqrt{2\frac{R}{\delta_{ij}}}tg\alpha)|_{-S^*}^{S^*} + O(\frac{\delta_{ij}}{R}),$$

where $O(\delta_{ij}/R) \to 0$ as $\delta_{ij}/R \to 0$.

Since S^* does not depend on δ_{ij}

$$arctg(2\sqrt{\frac{R}{\delta_{ij}}}tgS^*) = \frac{\pi}{2} + O(\frac{\delta_{ij}}{R})$$

and we obtain

$$g_{ij}^s = -\frac{1}{2} + \pi\sqrt{\frac{R}{\delta_{ij}}}(1 + O(\frac{\delta_{ij}}{R})) + O(\frac{\delta_{ij}}{R})$$

The term $\pi\sqrt{\frac{R}{\delta_{ij}}} = g_{ij}$, see formula (1.19), Section I with $R_i = R_j = R$, i.e. g_{ij} is the leading term is asymptotic expansion of g_{ij}^S as $\delta_{ij} \to 0$. The lemma is proved. Introduce the following quantity called the energy of the discrete network

$$E = \frac{1}{4}\sum_{i,j=1}^{N} g_{ij}(t_i - t_j)^2, \tag{2.67}$$

where $\{t_{ij}\}$ is the solution of the problem (1.24),(1.25), Section I (the factor $\frac{1}{4}$ have been discussed above). We need to show that the energy E grows as $O(\sqrt{\frac{R}{\delta}})$. Note that although each coefficient g_{ij} is of order $O(\sqrt{\frac{R}{\delta}})$ the differences $(t_i - t_j)^2$ may become small. Next lemma shows that this is not the case.

LEMMA 2.5. *The energy E of the discrete network is of order of $\sqrt{\frac{R}{\delta}}$, where $\delta = max_{ij}\delta_{ij}$. Here maximum is taken over all neighboring pairs (defined by Voronoi Tessellation).*

Proof. We shall employ the comparison method introduced in [21]. Define another network with the coefficients

$$g_{ij}^1 = \pi\sqrt{\frac{R}{\delta}} \text{ if } g_{ij} > 0,\ g_{ij}^1 = 0 \text{ if } g_{ij} = 0$$

Since $\delta = max\delta_{ij}$ we have $g_{ij} \geq g_{ij}^1$ and therefore

$$\sum_{i,j=1}^{N} g_{ij}x_ix_i \geq \sum_{i,j=1}^{N} g_{ij}^1 x_ix_i$$

Let $\{\tilde{t}_i\}$ be the solutions of the problem (1.24),(1.25), Section 1 and $\{\tilde{t}_i\}$ be the solutions of the problem (1.24),(1.25), Section 1, with the coefficients $\tilde{g}_{ij}$. The latter problem can be written as

$$\pi\sqrt{\frac{R}{\delta}}\sum(\tilde{t}_i-\tilde{t}_j)=0 \text{ for } i\in I\ ,\ t_i=\pm 1 \text{ for } i\in S^{\pm} \tag{2.68}$$

Here we sum over i,j such that $g^1_{ij}>0$ (i.e. over neighboring disks); I is the set of internal sites of the network, $S^{\pm}$ are boundary sites, the coefficients $g^1_{ij}=1$ if $g_{ij}>0$ and $g^1_{ij}=0$ if $g_{ij}=0$. The energy of the network $\{x_i,g_{ij}\}$ is greater than the energy of the network $\{\tilde{x}_i,\tilde{g}_{ij}\}$. Indeed, the energy in these networks is the minimum value of the following functionals

$$\sum_{i,j=1}^{N} g_{ij}(t_i-t_j)^2 \text{ and } \sum_{i,j=1}^{N} g^1_{ij}(t_i-t_j)^2$$

respectively.

Due to the above relation between the quadratic forms we have

$$\sum_{i,j=1}^{N} g_{ij}(t_i-t_j)^2 \geq \sum_{i,j=1}^{N} g^1_{ij}(t_i-t_j)^2 \geq \pi\sqrt{\frac{R}{\delta}}\sum(\tilde{t}_i-\tilde{t}_j)^2 \tag{2.69}$$

the last sum is taken over i,j such that $g^1_{ij}>0$.

Solution of the problem (2.68) does not depend on $\pi\sqrt{\frac{R}{\delta}}$ (we can cancel out $\pi\sqrt{\frac{R}{\delta}}$in the equation (2.68)). The LHS of (2.69) is $4E$ and its RHS is of the form $\pi\sqrt{\frac{R}{\delta}}const$, where the *const* does not depend δ and positive. Due to the uniform δ-close packing there exists a path $(i_k,i_{k+1}), k=1,...,K$ such that $g^1_{i_k,i_{\underline{k}=1}}=1$ and the disk $D_{i_1}\in S^+$ and a disk $D_{i_{K+1}}\in S^-$. It is impossible that all $\bar{t}_i-\bar{t}_j=0$ along this path. Thus the sum $\sum_{i,j=1}^{N}(\tilde{t}_i-\tilde{t}_j)^2$ is positive. The lemma is proved.

We briefly sketch here an alternative proof. First we show that the graph obtained by applying Voronoi construction (see above) is connected. Therefore there is a connected path from the top side of Π to its bottom side, which consists of M edges, and M is a finite number. Since the values of the potential on these sides are 1 and -1 respectively, the Kirchoff's law implies that $\sum_1^M(t_i-t_j)=2$. Then at least one term in this sum is greater than $2/M$, therefore it is not small and since the all coefficients are of order $O(\sqrt{\frac{R}{\delta}})$ lemma follows.

Using Lemma 2.4 , we can replace g^s_{ij} by g_{ij} as $\delta\to 0$ in (2.64). Then (2.63)-(2.64) provide the following bounds

$$\hat{A}\geq -\frac{1}{4}\sum_{i,j=1}^{N} g_{ij}(t_i-t_j)^2+(P^+ + P^-)+\sqrt{\frac{R}{\delta}}O(\delta/R) \tag{2.70}$$

$$\hat{A}\leq \frac{1}{4}\sum_{i,j=1}^{N} g_{ij}(t^-_i-t^-_j)^2+M+\sqrt{\frac{R}{\delta}}O(\delta/R), \tag{2.71}$$

M is uniformly bounded in δ as $\delta \to 0$.

The first two terms in (2.70) and the first term in (2.71) are the discrete analogs of the dual variational principles for the continuum medium. We have explained above how to replace $\frac{1}{4}$ by the usual $\frac{1}{2}$. It is known [14] that the values of the direct and the dual energy functionals for the continuum problem are the same when the exact minimizers are substituted into the functionals. Next Lemma is the discrete analog of this statement.

LEMMA 2.6. *The following equality holds*

$$\frac{1}{2}\sum_{i,j=1}^{N} g_{ij}(t_i - t_j)^2 = P^+ - P^- \tag{2.72}$$

where $\{t_i\}$ means solution of the problem (1.24),(1.25), Section 1.

Formula (2.72) differs from the usual Green's formula (for PDE) by the factor $\frac{1}{2}$. It appears due to the same the reason for as $\frac{1}{4}$ appears in the discrete formulas for energy presented above.

Proof. Following [8], we write (taking into account that $g_{ij} = g_{ji}$)

$$\frac{1}{2}\sum_{i,j=1}^{N} g_{ij}(t_i - t_j)^2 = \frac{1}{2}\sum_{i,j=1}^{N} g_{ij}(t_i - t_j)(t_i - t_j) =$$

$$\frac{1}{2}\sum_{i=1}^{N} g_{ij}t_i[\sum_{j=1}^{N} g_{ij}(t_i - t_j)] + \frac{1}{2}\sum_{j=1}^{N} g_{ij}t_j[\sum_{i=1}^{N} g_{ji}(t_j - t_i)] \tag{2.73}$$

The two sums in the square brackets are equal to zero due to (1.25), Section I (for $i \in I$ in the first sum and for $j \in I$ it the second sum). Then (2.73) becomes (only terms, which correspond to $S^{\mp}$ remain).

$$\sum_{i \in S^{\pm}} t_i \sum_{j=1}^{N} g_{ij}(t_i - t_j) \tag{2.74}$$

Note that $t_i = \pm 1$ for $i \in S^{\pm}$ in (2.74). Hence (2.74) is exactly equal to $P^+ + P^-$ and Lemma is proved.

The following Theorem shows that the continuum problem for the effective conductivity is asymptotically equivalent to the discrete network.

THEOREM 2.7. *Let the δ-close packing condition (see definition 2.3) hold.*
Then the effective coefficient (2.3)

$$\hat{A} = \frac{1}{2}\int_{Q_p} |\nabla\phi|^2 d\boldsymbol{x}$$

is given by the following asymptotic formula (as $\delta \to 0$):

$$\hat{A} = \frac{1}{4}\sum_{i,j=1}^{N} g_{ij}(t_i - t_j)^2 + \sqrt{\frac{R}{\delta}}O(\delta/R) + O(1), \tag{2.75}$$

where

$$g_{ij} = \pi\sqrt{\frac{R}{\delta_{ij}}}$$

and $\{t_i, i = 1, ..., N\}$ *is solution of the discrete network problem (1.24),(1.25).*

The leading term $\frac{1}{4}\sum_{i,j=1}^{N} g_{ij}(t_i - t_j)^2$ *is of order* $\sqrt{R/\delta}$ *and is expressed through the solution of the discrete network problem (1.24), (1.25), Section 1.*

Proof. Using (2.70),(2.71) and (2.72) we obtain

$$\begin{aligned} &\frac{1}{4}\sum_{i,j=1}^{N} g_{ij}(t_i - t_j)^2 + \sqrt{\frac{R}{\delta}}O(\delta/R) \leq \hat{A} \\ &\leq \frac{1}{4}\sum_{i,j=1}^{N} g_{ij}(t_i - t_j)^2 + M + \sqrt{\frac{R}{\delta}}O(\delta/R) \end{aligned} \tag{2.76}$$

By Lemma 2.5 the term $\frac{1}{4}\sum_{i,j=1}^{N} g_{ij}(t_i - t_j)^2$ in (2.76) is of the order $\sqrt{\frac{R}{\delta}}$ and, consequently, it is the leading term in asymptotic expansion.

REMARK 2.8. *Our proof can be modified so that the remainder in the asymptotic formula (2.75) can be evaluated in explicit terms. The latter allows to obtain the error estimate of our networks approximation. These results will be presented in the forthcoming work [7]*

Conclusions. In this work we start with a class of physically interesting problems, formulate them carefully, establish a mathematically rigorous approximation, use it for numerical computations and then draw physical conclusions.

At present, there are two rigorous mathematical network approximations for modeling continuum high contrast media.

The Borcea-Kozlov-Papanicolaou model ([9] and references therein) was developed for the high contrast continuum problems arising in imaging, when the materials properties are not known and it is convenient to model the high contrast in a simple geometric manner by using the Kozlov's function $\epsilon^{S(X)/\epsilon}$. The two key parameters in this model are $\sqrt{k_+/k_-}$ (determine the conductivity of the edges in the network), where k_+ and k_- are the principal curvatures in the saddle points of $S(x)$ and the high contrast parameter ϵ.

Our model has been developed for the analysis of the two phase composites, when the materials properties of each phase and the geometry (e.g. the shapes of particles) are known. The contrast ratio is taken to be infinite, and it does not contain the saddle points and the curvatures. The key mathematical parameter in our model is the relative interparticle distance. Similar parameters have been used in physics and mechanics of composites, and they can be observed and measured in actual experiments (see, for example, [43]).

For periodic (e.g.square) arrays this parameter amounts to the critical concentration in "almost touching" regime and is uniquely determined by the critical volume fraction [20]. We have shown that this parameter can be introduced for non periodic arrays, when it is not uniquely determined by the volume fraction. Also, while in the periodic arrays "almost touching" conductivity appears in the volume fractions which are close to the maximal, the irregular (random) arrays may have conducting chains

with very small relative interparticle distance even when the volume fraction of the particles is not very close to the maximal.

We further note that various mathematical techniques have been used for the study of the "almost touching case" for various periodic arrays ([29], [30], [6]). The case of the full touching has been investigated in [31]. Our approach utilizes the ideas developed in [20] and can be used for mathematical justification of the asymptotic formulas obtained in [20]. In a loose sense our work presents a "randomization" of the Keller's model.

Finally, we mention that in the present work we implemented numerically the network approximation. For the monodispersed composites we recovered classical percolation picture and showed that this approximation is an efficient computational tool. For a polydispersed composite we found a pronounced effect in the behavior of the effective conductivity. This suggests that the high contrast, densely packed composites are very attractive for the design of new materials.

Acknowledgments. The work of L. Berlyand was supported by NSF grant DMS-9971999. Part of this work was done when A. Kolpakov visited L. Berlyand at Penn State. He is grateful for the hospitality and support of his visit. We are grateful to E. Khruslov for useful discussions on Voronoi tesselation. We are also grateful to L. Borcea for providing us with a number of references and to K. Bhattacharya, L. Borcea and A. Novikov for suggestions which lead to an improvement of the presentation.

REFERENCES

[1] Ambegaokar, V., Halperin, B.I., Langer, J,S. 1971, *Hopping conductivity in disordered systems*, Phys.Rev.B, 4(8), pp2612-2620 (1971).
[2] Babushka, I. Anderson, B., Smith, P., and Levin K. *Damage analysis of fiber composites.* Preprint
[3] Bakhvalov N. S., Pansenko G. P.,*Homogenization of Process in Periodic Media*, Kluwer, Dordrecht/Boston/London (1989).
[4] Bensoussan A., Lions J-L., Papanicolaou G., *Asymptotic Analysis for Periodic Structures*, North-Holland, Amsterdam (1978).
[5] Berlyand, L. V., A. D. Okhotsimskii, A. D., *An average description of an elastic medium with a large number of small absolutely by rigid inclusions.* Soviet Phys. Dokl. 28 (1):81–84 (1983).
[6] Berlyand,L.V. and Mityushev V. *Generalized Clausius-Mossotti Formula for Random Composite with Circular Fibers*, Journ. Stat. Phys. 102, 1/2 pp. 115-145 (2001).
[7] Berlyand, L.V., Novikov *Error estimate for the discrete network approximation for densly packed high contrast composites.* In preparation.
[8] Borcea L., Berrymen J.G., Papanicolaou G., *Matching pursuit for imaging high contrast conductivity.* To appear in Inverse Problems.
[9] Borcea, L., Papanicolaou G., *Network approximation for transport properties of high contrast materials.* SIAM J Appl Math, 58(2), pp.501-539 (1998).
[10] Brown, *Dielectrics* .,Springer-Verlag. Berlin.(1956).
[11] Bruno, O., *The effective conductivity of strongly heterogeneous composites.* Proc. Royal Soc. London A, pp. 353-381 (1991).
[12] Clerc, J.P., Giraud, G., Laugier, J.M., Luck, J.M., *The electrical conductivity of binary disordered systems, percolation clusters, fractals and related models*, Advanced in Physics, 39(3), pp. 191-309 (1990).
[13] Dykne, *Conductivity of two dimensional two-phase system.* JETP, 32, pp.63-65 (1971).
[14] Ekeland, I., Temam, R.*Convex Analysis and Variational Problems.*, North Holland (1976).
[15] Cheng, H., Greengard, L., *A method of images for the evaluation of electrostatic fields in systems of closely spaced conducting cylinders.* SIAM J. Appl. Math., 50:1, pp 122-141 (1998).

[16] Golden, K. M., *Percolation models for porous media*, in Homogenization and porous medium, U. Hornung,ed., Springer Verlag (1997).
[17] Halperin, B.I.,*Remarks on percolation and transport in networks with a wide range of bond strengths*, Physica D, 38, pp 179-183 (1989) .
[18] Hill, R.,*Characterization of thermally conductive epoxy composite fillers.*, Proc. Thechnicla Programm "Emerging Packing Technology" , at the Surface Mount Technology Association Symp. held at Research Triangle Park, NC, November, 18-21, pp 125-131 (1996) .
[19] Grimmett, G. *Percolation*,Springer Verlag (1989).
[20] Keller, J.B., *Conductivity of a Medium Containing a Dense Array of Perfectly Conducting Spheres or Cylinders or Nonconducting cylinders.* J. Appl. Phys., 34:4, pp 991-993 (1963).
[21] Kesten, H., *Percolation theory for mathematicians.* Birkhauser. Boston, Basel, Stuttgart. (1992).
[22] Koplik, J., *Greeping flow in two-dimensional networks.* J. Fluid Mech., Vol.119, pp 219-247 (1982).
[23] Kozlov, S. M., *Averaging of random operators.* Matem. Sbornik, 109(2): 1979, pp 188–203 (English Transl.: Math USSR, Sb.37:2, pp167-180 (1980)).
[24] Kozlov, S.M., *Geometrical aspects of averaging*, Russ. Math. Surveys, 44:22, pp 91-144 (1989).
[25] Kuchling H. *Physics* , VEB Vachbuchverlag, Leipzig (1980).
[26] G. Lubin, editor, *Handbook of composites,* V.1, Van Reinhold Co Inc.(1982)
[27] Maz'ya, V.G., Nazarov, S.A. and Plamenevskii, B.A. *Dirichlet problem in domains with small bridges.* Sibirskii Mat.Zhurnal, Vol 25 , No 2, pp. 161-179,(1984)
[28] Milton, G.W. *Mechanics of Composites*, Camdridge University Press (to appear), (2000).
[29] McPhedran, R. *Transport property of cylinder pairs of the square array of cylinders*, Proc. R. Soc. London, AA408 (1986), pp.31-43.
[30] McPhedran, R., Poladian.L, and Milton, G.W. *Asymptotic studies of closely spaced, highly conducting cylinders*,Proc.. R. Soc. Lond.A, 415, pp.185-196 (1988).
[31] McPhedran, R., Milton, G.W. *Transport properties of touching cylinder pairs and of the square array of touching cylinders.*
[32] McLachlan, D., Blaszkiewicz, M., Newnham,.R. *Electrical Resistivity of Composites.* J. Am. Ceram. Soc., 73 (8) 2187-2203 (1990).
[33] Meester R., Roy R., *Continuum percolation* Cambridge Iniversity Press (1996).
[34] Papanicolaou, G., Varadhan, S. *Boundary value problems with rapidly oscillating random coefficients,* Colloquia Mathematica Societatis Janos Bolyai 27, Radon Fields, Esztergom (Hungary), 1979, pp. 835-873.
[35] Schawartz, L.M., Banavar, J.R., Halperin, B.I., *Biased-diffusion calculations of effective transport in inhomogeneous continuum systems*, Physical review B, Vol.40, 13, pp 9155-9161 (1989).
[36] Shah, C.B., Yortsos, Y.C.,*The permiability of strongly-disordered systems, Physics of Fluids*, Vol.8, No.1, pp 280-282 (1996)
[37] Smythe, W. R., *Static and dynamic electricity.* 2nd edition, McGraw-Hill, NY, Toronto, London, 1950.
[38] Stauffer D. and Aharony A., *Introduction to percolation theory*, Taylor and Francis, London (1992).
[39] Tamm I. E. *The theory of electricity.* Nauka, Moskow (1976).
[40] Thovert, J. F., Kim, I. C., Torquato,S., and Acrivo, A., *Bounds on the effective properties of polydispersed suspensions of spheres. An evaluation of two relevant morphological parameters,* J. Appl. Phys., 67, pp. 6088-6098 (1990).
[41] Van Fo Fi, G.A.,. *Structures made of reinforced plastics.* Tehnika, Kiev (1971) (in Russian).
[42] Li, Y.Y. and Vogelius, M., *Gradient estimates for solutions to divergence form elliptic equations with discontinuous coefficients.* To appear Arch. Rational Mech. and Anal.
[43] Wu, S.*Phase structure and adhesion in polymer blends:A criterion for rubber toughening*,Polymer, 26 (1985),pp. 1855-1863.

Appendix 1: Lower bounds for $|BC|$ and $|AB|$.

The lower bound on $|BC|$ follows from simple geometrical considerations. On figure 2.7 for a fixed neck-length $2S$ between the disks centered at O and O' the length $|BC|$ is the smallest if the third disk centered at Q touches the other two. Consider the right triangle ΔOPQ. By the Pyhagorean theorem

$$|PQ| = S + |BC| + |CQ| = \sqrt{(2R)^2 - (R + \delta/2)^2},\ S = |PB|$$

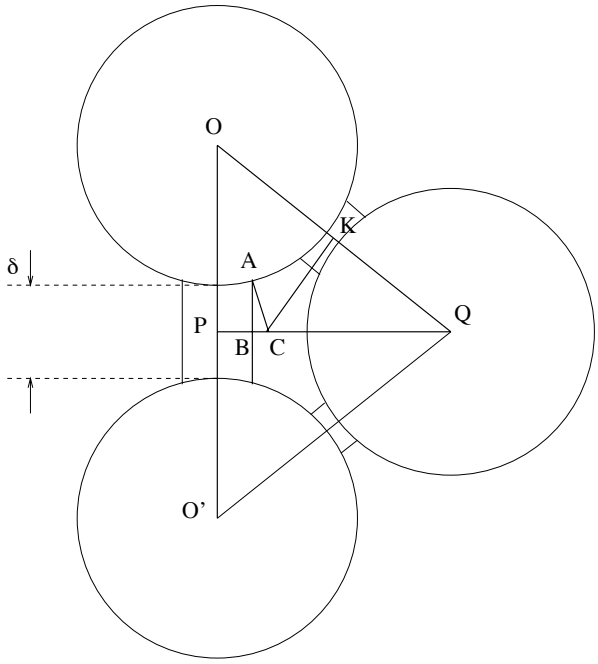

FIG. 2.7.

also

$$\frac{|OK|}{|CQ|} = \frac{R}{|CQ|} = \frac{\sqrt{(2R)^2 - (R+\delta/2)^2}}{2R} = |PQ|/|OQ| = \cos(\angle OQP)$$

therefore

$$|BC| = \frac{R^2 - R\delta - \delta^2/4}{\sqrt{3R^2 - R\delta - \delta^2/4}} - S. \tag{2.77}$$

An independent of δ upper bound on S follows if we consider the same three disks when all of them touch each other and they are connected by identical in width necks (see figure 2.8). In this case we have

$$S + |BC| = |PC|,$$

Then considering the right triangle ΔABC, we have $|BC| = 1/2|AC|$ and $|PC| = 1/3|PQ|$ from the equilateral triangle OQO. Thus

$$S + \frac{1}{2}|AC| = \frac{1}{3}|PQ|,$$

$$S + \frac{1}{2}(|OC| - R) = \frac{1}{3}\sqrt{3}R,$$

$$S + \frac{1}{2}(\frac{2}{3}|PQ| - R) = \frac{1}{3}\sqrt{3}R,$$

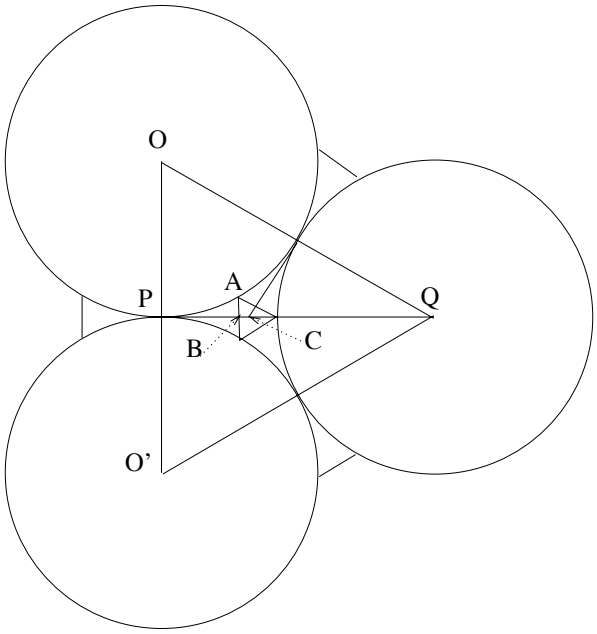

FIG. 2.8.

Since $|PQ| = \sqrt{3}R$

$$S = \frac{R}{2}. \tag{2.78}$$

Combining (2.77) and (2.78) for sufficiently small δ we have

$$|BC| \geq \frac{R^2 - R\delta - \delta^2/4}{\sqrt{3R^2 - R\delta - \delta^2/4}} - \frac{R}{2} > \frac{3}{40}R. \tag{2.79}$$

The lower bound on $|AB|$ is found when the disks centered at O and O' touch each other ($\delta = 0$). We have

$$|AB| = |OP| - |OA|\cos(\angle POA) = R - \sqrt{R^2 - S^2}. \tag{2.80}$$

Combining (2.80) with the upper bound on S given by (2.78) we arrive at a lower bound on $|AB|$ which does not depend on δ